JASN

J Am Soc Nephrol. 2018 Mar; 29(3): 841–856.
Published online 2017 Nov 27.
doi: 10.1681/ASN.2017040409: 10.1681/ASN.2017040409

PMCID: PMC5827593
PMID: 29180395

Tamm-Horsfall Protein Regulates Mononuclear Phagocytes in the Kidney

Radmila Micanovic,[1] Shehnaz Khan,[1] Danielle Janosevic,[1] Maya E. Lee,[1] Takashi Hato,[1] Edward F. Srour,[1,2] Seth Winfree,[1] Joydeep Ghosh,[1] Yan Tong,[3] Susan E. Rice,[1] Pierre C. Dagher,[1,4] Xue-Ru Wu,[5] and Tarek M. El-Achkar[1,4]

[1]Departments of Medicine,
[2]Microbiology and Immunology, and
[3]Biostatistics, Indiana University, Indianapolis, Indiana;
[4]Department of Medicine, Roudebush Veterans Affairs Medical Center, Indianapolis, Indiana; and
[5]Departments of Urology and Pathology, New York University and Manhattan Veterans Affairs, New York, New York
Corresponding author.
Correspondence: Dr. Tarek M. El-Achkar (Ashkar), Division of Nephrology, Indiana University School of Medicine, 950 W Walnut, R2 E280, Indianapolis, IN 46202. Email: telachka@iu.edu

Received 2017 Apr 12; Accepted 2017 Nov 1.

Abstract

Tamm–Horsfall protein (THP), also known as uromodulin, is a kidney-specific protein produced by cells of the thick ascending limb of the loop of Henle. Although predominantly secreted apically into the urine, where it becomes highly polymerized, THP is also released basolaterally, toward the interstitium and circulation, to inhibit tubular inflammatory signaling. Whether, through this latter route, THP can also regulate the function of renal interstitial mononuclear phagocytes (MPCs) remains unclear, however. Here, we show that THP is primarily in a monomeric form in human serum. Compared with wild-type mice, $THP^{-/-}$ mice had markedly fewer MPCs in the kidney. A nonpolymerizing, truncated form of THP stimulated the proliferation of human macrophage cells in culture and partially restored the number of kidney MPCs when administered to $THP^{-/-}$ mice. Furthermore, resident renal MPCs had impaired phagocytic activity in the absence of THP. After ischemia-reperfusion injury, $THP^{-/-}$ mice, compared with wild-type mice, exhibited aggravated injury and an impaired transition of renal macrophages toward an M2 healing phenotype. However, treatment of $THP^{-/-}$ mice with truncated THP after ischemia-reperfusion injury mitigated the worsening of AKI. Taken together, our data suggest that interstitial THP positively regulates mononuclear phagocyte number, plasticity, and phagocytic activity. In addition to the effect of THP on the epithelium and granulopoiesis, this new immunomodulatory role could explain the protection conferred by THP during AKI.

Keywords: macrophages, acute renal failure, ischemia-reperfusion

Abstract

Tamm–Horsfall protein (THP), also known as uromodulin, is a glycoprotein uniquely expressed in the kidney, by cells of the thick ascending limb (TAL) of the loop of Henle.[1–3] THP is predominantly sorted to the apex of TAL cells, and secreted into the urine as one of the most abundant urinary proteins. However, a small amount of THP is also released basolaterally toward the interstitium and the circulation.[1,4,5] The structure and functions of basolaterally released THP are not fully understood. We previously showed that interstitial THP directly interacts with the basolateral domain of S3 segments, where it mediates a protective crosstalk between S3 segments and TAL.[5–7] This interaction results in the downregulation of inflammatory signaling in S3 cells during AKI. Indeed, $THP^{-/-}$ mice are more prone to AKI, and have heightened inflammation and neutrophil infiltration.[7–9] THP deficiency also causes delayed kidney recovery after injury.[5] Our ongoing research is focused on identifying specific receptors on S3 segments that mediate this signaling. However, it is also possible that basolaterally released THP interacts with other cell types in the renal interstitial space.[1]

The renal interstitium is a rich milieu that harbors various cells types.[10] Resident and infiltrating mononuclear phagocytic cells (MPCs) form an important immune surveillance network, which can modulate various functions in health and disease.[11–13] It has been proposed that THP has immunomodulatory functions, but the exact role of THP in regulating the functions of renal immune cells, specifically renal MPCs, is still unclear. Earlier works of Muchmore and Decker[14] and Hession *et al.*[15] found THP to be suppressive of inflammation by binding to immune cells or cytokines. Subsequent studies, however, supported a proinflammatory function of THP, through activation of immune cells such as neutrophils, monocytes, and dendritic cells.[16–21] These conflicting observations could be explained by the fact that all of the previous studies were performed *in vitro* or *ex vivo*, utilizing for the most part aggregated forms of THP that could be highly immunogenic.[22] This may not accurately reflect interstitial or circulating THP, which is unlikely to be highly aggregated. In addition, in light of our improved understanding of the complex relationship between inflammation and appropriate versus maladaptive healing, we now appreciate that a controlled inflammatory response is not deleterious. Rather, pathologic conditions occur when inflammation fails to terminate.[23–27] This maladaptive process typically leads to abnormal healing, chronic inflammation, and fibrosis. This particularly pertains to renal MPCs and their complex role in maintaining health and transitioning into appropriate healing from injury.[28–31]

Proper MPC function is important for the clearance of danger-associated molecular patterns (DAMPs) and pathogen-associated molecular patterns.[24,28,30,31] MPCs are also essential for the clearance of neutrophils from injured organs.[32–34] All of these functions are necessary to prevent persistent inflammatory response, and usher adaptive healing and recovery. This pleiotropic role of MPCs has become increasingly recognized, and several macrophage phenotypes associated with progression of injury and/or repair have been described.[11,29–31,35,36] In addition, the homeostasis of MPCs needs to be properly maintained both spatially and temporally, in order to ascertain a timely transition from an injury to a healing phenotype.[37] Notwithstanding the recent progress, there is still a significant gap in our knowledge of the exact interplay between the plasticity of macrophages and the divergent pathophysiologic manifestations, particularly in a renal context. It is of note that, in this work, we use the term MPCs because there is a large degree of overlap existing between macrophages and dendritic cells.[38–40]

The role of THP in modulating the immune system *in vivo* has not been studied in detail.[10] Our previous work with $THP^{-/-}$ mice suggests that THP deficiency is associated with a maladaptive response to injury and persistent inflammation.[5,7,9] On the basis of this, we investigated the hypothesis that THP is an important positive regulator of renal MPC function in health and after AKI. This role of THP could augment the anti-inflammatory effect exerted on the S3 epithelium,[6,41] collectively aiming to terminate inflammation and enable timely transition into healthy recovery.

Results

Characterization of Human THP in the Circulation/Renal Interstitium Compared with Urine

THP is secreted in the urine from the apical domain of TAL as a highly aggregated polymer with molecular mass exceeding a million Daltons.[2,42] This is demonstrated by the fact that, under native conditions, urinary THP will not enter a gel to undergo electrophoresis (Figure 1A, lane a); however, when applying denaturing and reducing conditions, urinary THP will migrate predominantly in the 85–90 kD region (Figure 1B, lane a), which corresponds to the molecular mass of full-length glycosylated THP.[42] Highly aggregated proteins are typically immunogenic. Therefore, we hypothesized that basolaterally released THP, which makes its way to the interstitium and circulation, is not aggregated. Because the isolation of pure interstitial THP is not feasible, we characterized serum (circulating) THP, as a surrogate to the renal interstitial form of THP. Under denaturing and reducing conditions, THP from human serum has a molecular mass around 85–90 kD, which is comparable to that of full-length urinary THP (Figure 2, lanes a–c). Using size exclusion chromatography, we isolated different molecular mass fractions of normal human serum and performed western blot after immuno-precipitating THP in each fraction. The fraction that harbored the majority of THP corresponded to proteins in the range of 44 and 158 kD, and contained a single band in the 80–90 kD region (Figure 2, lanes d–g). This can only be interpreted that the predominant form of THP in the circulation and, by extension, in the interstitium of the kidney, is a full-length monomeric form.

Although THP in the urine is highly aggregated and predominantly in its full-length form (Figure 1, A and B, lanes a and e), a low abundance, truncated, and nonaggregating form of THP (tTHP) can be reproducibly isolated from human urine after treatment with urea and subsequent size exclusion chromatography (Figure 1, A and B, lanes b–d). tTHP will only dimerize under native conditions, and will not polymerize even if subjected to increasing concentrations of salt (Supplemental Figure 1). Proteomic characterization of tTHP shows that the truncation occurs at the level of the interlinker domain within the zona pellucida (ZP) region,[2,43–45] between ZP-N and ZP-C subdomains (Figure 1, C and D). The ZP domain confers to THP its aggregating properties.[43,45] Therefore, the location of the truncation and the loss of ZP-C could partially explain why tTHP does not assemble beyond a dimer and aggregate. Because tTHP is similar to circulating/interstitial THP in that it does not polymerize to highly aggregated complexes, and it retains the domains that are likely involved in functional activity (Figure 1D), we used it in subsequent experiments as an alternative for circulating/interstitial THP; the latter cannot be purified due to its very low concentration.

THP Colocalizes with Resident MPCs in the Renal Interstitium

To determine if THP interacts with renal immune cells, we performed immunofluorescence confocal microscopy on kidney sections labeled with THP and CD11c, a marker for resident MPCs.[11] THP colocalizes with a substantial number of $CD11c^{+}$ cells, as shown in Figure 3, A and B. This finding was also confirmed by immuno-electron microscopy for THP, whereby gold-labeled THP was observed within mononuclear cells (Figure 3C). Quantitative three-dimensional (3D) tissue cytometry[46] was used to determine that 14.0%±2.4% of $CD11c^{+}$ cells also have significant THP staining (Supplemental Figure 2).

Resident MPC Number Is Decreased in the Kidneys but Not Liver of $THP^{-/-}$ Mice

We performed immuno-histochemistry for F4/80, a specific marker for murine MPCs, on kidney sections from $THP^{-/-}$ and $THP^{+/+}$ mice. Figure 4 shows that $F4/80^{+}$ renal macrophages are decreased in $THP^{-/-}$ outer medulla, especially the inner stripe, compared with $THP^{+/+}$ kidney sections. This decrease in renal MPCs was also demonstrated using flow cytometry (Figure 5). Using multisurface marker labeling, we

determined that THP deficiency predominantly affected the CD11b high (hi), F4/80^{+} population (also in Supplemental Figure 3 on the basis of reference[38]). A distinct population that was CD11b low (lo), F4/80 hi, and MHCII hi, believed to arise from distinct ontogeny,[38,47] was not affected. In the liver, another parenchymal organ, the number of resident macrophages was not changed in THP$^{-/-}$ compared with THP$^{+/+}$ mice (Supplemental Figure 4). These findings support that THP is an important determinant of the number of MPCs specifically in the kidney, because this effect was not observed in the liver.

THP Causes Macrophage Proliferation and Activation of Akt

To investigate the possible mechanisms underlying the effect of THP on MPCs, we examined the effect of tTHP on the proliferation of human monocytic/macrophage SC cells in culture. tTHP causes a time- and dose-dependent increase in macrophage numbers (Figure 6, A and B) compared with control conditions. Interestingly, the increase in the number of these cells was not associated with inhibition of apoptosis, as shown using a propidium iodide (PI)/annexin V flow-based assay. There was also no difference in PI^{+} cells in control versus tTHP treated, (15.4%±1.2% versus 14.9%±0.4%, respectively; P=0.8). We also studied the main signaling pathways associated with cell proliferation, and found that Akt, but not Erk or NF-κB pathways, was activated by THP. Cumulatively, these data suggested that THP stimulates the proliferation of MPCs, and that this effect could be associated with the activation of Akt.

Exogenous Administration of tTHP Increases Resident Renal Mononuclear Phagocytes in THP$^{-/-}$ Mice

To verify that systemic administration of THP reaches kidney MPCs, we used intravital imaging of CX3CR1-EGFP mouse kidneys, where resident MPCs endogenously express GFP (Figure 7A).[48] tTHP was labeled with Alexa 568 and administered intravenously. Within 30 minutes, tTHP was detected in the peritubular circulation and at the basolateral domain of proximal tubules (not shown). At 60 minutes and onward, tTHP colocalized with renal MPCs in both sessile dendritic-looking cells and in mobile sphere-like cells, which have the characteristic appearance of macrophages (Figure 7, B and C, Supplemental Video 1). Flow cytometry analysis at 60 minutes showed that 17.2%±0.8% of CX3CR1^{+} cells were THP positive, thereby confirming the findings of intravital imaging. The labeling of CX3CR1-negative leukocytes with THP was significantly less (7.5%±0.5%; P<0.05 compared with THP^{+}, CX3CR1^{+} cells, data not shown).

Subsequently, to investigate if exogenously administered THP can reverse the reduction in MPC abundance observed in THP$^{-/-}$ kidneys, we studied the effect of treatment with tTHP on the number of renal MPCs in these mice. tTHP was administered intraperitoneally (IP) daily for 6 days and then flow cytometry was performed on kidneys from THP$^{-/-}$ mice compared with controls. Figure 7, D and E, shows that tTHP administration increased the number of renal MPCs, specifically the CD11b hi population that was reduced in Figure 5, but did not affect the CD11b low population described earlier (also Supplemental Figures 5 and 6). Interestingly, within the CD11b hi population, THP treatment shifted this population toward MHCII positivity (decrease in MHCII-negative and increase in MHCII-positive cells). This suggests an added effect of THP on the maturation and/or the plasticity of resident renal MPCs.

THP Enhances the Phagocytic Activity of MPCs *In Vivo*

To examine if THP affects MPC activity *in vivo*, we used two complementary approaches. First, we systemically administered liposomes with clodronate versus empty liposomes to THP$^{+/+}$ versus THP$^{-/-}$ mice. Liposomes are readily phagocytosed by MPCs. In the case of liposomal clodronate, successful phagocytosis will lead to intracellular release of clodronate and MPC death.[49] Therefore, the degree of macrophage depletion with liposomal clodronate, compared with empty liposomes, is a surrogate measure of the phagocytic activity of MPCs *in vivo*. Figure 8 shows that, compared with empty liposomes,

clodronate-filled liposomes led to almost complete depletion of F4/80 MPCs in the cortex of $THP^{+/+}$ kidneys. A significant, albeit less robust, depletion of MPCs was also observed in the outer medulla of these kidneys. In $THP^{-/-}$ kidneys, there was a significant reduction in the degree of MPC depletion with clodronate compared with $THP^{+/+}$ kidneys in all compartments of the kidney, especially in the outer medulla. These findings suggest THP deficiency causes an impairment in the phagocytic ability of MPCs, which could explain the observed resistance to the depleting effect of liposomal clodronate in $THP^{-/-}$ kidneys.

The second approach was to directly measure the phagocytic activity *in vivo* by measuring the uptake of systemically injected fluorescent beads by renal MPCs, as recently demonstrated by Stamatiades *et al.*[50] and in Supplemental Figure 7. We used 3D tissue cytometry, as described recently,[46] to quantify bead uptake in the cortex, outer stripe, and inner stripe (Figure 8, D–F). Our results show that bead uptake by MPCs was significantly reduced in $THP^{-/-}$ cortex and inner stripe, but not the outer stripe.

Taken together, the two approaches confirm the role of THP in the phagocytic activity of MPCs. The observation of reduced phagocytic activity in the cortex of $THP^{-/-}$ kidneys, despite no reduction in the number of MPCs in that area compared with $THP^{+/+}$, demonstrates that the effect of THP on phagocytosis is independent from its role in regulating MPC abundance.

Myeloid Cell Dynamics Are Impaired during AKI

To understand the relevance of the regulatory effect of THP on macrophages in the setting of AKI, we studied the distribution of immune cells in the kidneys of $THP^{+/+}$ and $THP^{-/-}$ mice using flow cytometry (Figure 9) after sham or ischemia-reperfusion injury (IRI) surgeries. $THP^{-/-}$ mice are prone to kidney injury, as shown by the changes in serum creatinine (Supplemental Figure 8), which is consistent with our previous findings.[5,7,9] The absence of THP caused a shift toward a proneutrophilic phenotype in sham and after IRI. There was a relative deficiency of MPCs defined by $CD11b^{+}$, $Ly6G^{-}$ cells (see also Supplemental Figure 9 for further subclassification), which became even more aggravated after AKI (Figure 9B). There was no significant difference in nonmyeloid cells between the two strains of mice (defined as $CD45^{+}$, $CD11b^{-}$) during AKI.

Impaired Macrophage Phenotype Switching in $THP^{-/-}$ Kidneys during AKI

To better characterize the signaling associated with MPC activity in AKI, we measured the changes in 32 cytokines, chemokines, and growth factors at various time points after AKI compared with sham, in kidneys from $THP^{-/-}$ and $THP^{+/+}$ mice, using a multiplex ELISA assay (Figure 10A). In $THP^{+/+}$, chemokines and growth factors involved in regulating the chemotaxis and activation of neutrophils and macrophages increase at 6 through 24 hours after IRI. Increase in other proinflammatory/M1 cytokines is also evident. At 48 hours post-IRI, $THP^{+/+}$ kidneys show persistent macrophage chemokine and growth factor signaling, and heightened M1/Th1 signaling, but also a significant surge in repair/M2 cytokine levels. In contrast, in $THP^{-/-}$ mice, proneutrophilic signaling and inflammatory/M1 signaling is dominant 6–24 hours post-IRI. Macrophage chemokine and growth factor signaling is suppressed at the early time points and is not apparent until 48 hours postinjury. Most notably, repair M2 signaling, that was a prominent feature of $THP^{+/+}$ at 48 hours, is not activated in $THP^{-/-}$ mice.

These findings not only suggest dysfunctional signaling involved in macrophage activation in $THP^{-/-}$ kidneys after AKI, but also reveal a new observation of impaired signaling needed in repair and switching from M1 to an M2 macrophage phenotype. Indeed, flow cytometry on kidneys 48 hours after IRI in $THP^{+/+}$ and $THP^{-/-}$ confirmed that $THP^{-/-}$ kidneys have lower $CD206^{+}$ (M2) and higher $CD86^{+}$, $CD206^{-}$ (M1) macrophage distribution (Figure 10B). Of note, all $CD206^{+}$ macrophages are also positive for CD86,

suggesting an M1 to an M2 phenotypic switch rather than the appearance of *de novo* M2 phenotype.

Rescue of THP$^{-/-}$ Mice after AKI by Administration of tTHP

Because THP deficiency is associated with a proinflammatory phenotype, impaired macrophage repair signaling, and worsened kidney injury, we next aimed to investigate whether tTHP administration after AKI could attenuate the injury in the setting of THP deficiency (Figure 11). We treated THP$^{-/-}$ mice with tTHP or vehicle, 24 hours after IRI, and followed the course of kidney injury until 72 hours. These mice were resuscitated with daily 1 cc of saline, to mimic a clinical setting. Figure 11 shows that the two groups of mice had a comparable degree of injury, as measured by their serum Cr and NGAL levels at 24 hours after IRI. THP$^{-/-}$ mice treated with tTHP at 24 hours after IRI had an improvement in the course of AKI at 48–72 hours, both using functional (serum Cr) and injury (NGAL) markers (Figure 11, A and B), compared with vehicle-treated mice. The protection conferred by THP treatment was also confirmed by histologic assessment of injury (Figure 11, C and D), and by reduction in NGAL mRNA (Figure 11E), which is transcriptionally activated by injury.[51] We also observed an increase in the number of CD206^{+} macrophages in kidneys from the THP treatment group (Figure 11, F and G), which is consistent with findings from Figure 10, and underscores the importance of THP in phenotypic switching of macrophages, that could partially explain the protection conferred by THP.

Discussion

The role of THP, particularly as an immunomodulator, has been a subject of controversy over the last several decades.[1] In this work, we show for the first time that THP regulates the number and activity of kidney mononuclear phagocytes *in vivo*. To our knowledge, this is the first report that studied extensively the immunomodulatory effect of THP *in vivo*. Furthermore, we also show the importance of this effect in the setting of kidney injury. These findings are essential to advance our understanding of THP biology, its role in kidney health, and its importance in modulating a protective effect in kidney injury. They also complement our previous work on the protective effect of THP on inflammatory signaling in the epithelium.[5,7,9] Therefore, THP emerges as a multifaceted protein with pleiotropic effects on different types of cells. In addition, we showed for the first time that exogenous monomeric THP administration after AKI could improve the course of injury. This could have implications on the use of THP as a therapeutic agent in the treatment of AKI.

That THP is monomeric in the circulation/interstitium is a novel finding that will promote our understanding of THP biology. THP in the urine is predominantly multimeric, and aggregates due to its ZP domains.[2] It is unclear why circulating THP, despite being full-length, does not aggregate. This could be partially due to its low concentration in the serum (range, 20–50 ng/ml) compared with urine (range, 20–50 μg/ml). Another explanation could be a sequence difference at the C-terminus that interferes with the properties of the ZP, thereby inhibiting aggregation, similar to what was shown by Rampoldi and colleagues[43–45] in cell culture models; this area requires further investigation. The release by the kidney of a monomeric THP in the interstitium and circulation is very intriguing, as more data are accumulating about the correlation of serum THP with kidney function and other systemic diseases.[52–54] We therefore propose that monomeric THP released by the kidney is an important regulator of crosstalk between various cells within the kidney, and possibly between the kidney and other organs—a sort of "kidney stress hormone."

It is unclear whether a full-length form of nonaggregating monomeric THP is also secreted in the urine. In this study, we isolated from the urine a truncated form of THP that lacks one ZP subdomain, but retains all of the other highly conserved domains. Because of this truncation, this form does not aggregate, but can only dimerize at higher concentrations. The nature of this dimerization and the THP domains involved in it

are unclear, but such a process has been reported with other proteins harboring EGF-like domains,[53] or could be due to the remaining ZPN domain.[56,57] Isolation of a nonaggregating monomeric form of THP from the urine after treatment with urea is consistent with similar previous findings by Serafini-Cessi.[58] We also propose that this truncation is a result of urinary proteolysis and/or handling, which may not necessarily be physiologically relevant in the urine, but is advantageous in isolating a monomeric form of THP as we have shown.

The finding that THP regulates the number of kidney MPCs is novel, and ushers a new understanding of tubular-immune cell crosstalk.[6,10] The reduction of MPC number in THP$^{-/-}$ mice occurs predominantly in the outer medulla, an area with high TAL density and conceivably high THP interstitial concentration.[4] The data on SC cells support an effect of THP on proliferation, possibly through activation of Akt. Administration of THP systemically over 6 days increased the number of MPCs in THP$^{-/-}$ kidneys. Although we did not investigate renal MPC proliferation *in vivo*, it is also possible that THP administration will increase monocyte migration and differentiation within the kidney. This is the subject of ongoing investigations in our laboratory.

The depletion of MPCs in THP$^{-/-}$ kidneys is specific to a subpopulation (CD11b hi, F4/80^{+}) in the outer medulla. In THP$^{+/+}$, this population of cells is more abundant in the medulla compared with the cortex (Supplemental Figure 10). The implications for these findings are unclear, but mounting evidence supports that MPCs within the kidney perform specialized functions (such as specific antigen recognition and rejection) in a regional distribution.[59,60] This could suggest that the presence of THP may be important in regulating specific functions of the renal mononuclear phagocytic system in the outer medulla. The added finding that THP also regulates the phagocytic activity of MPCs, as shown in Figure 8, also supports such a proposition, and underscores the importance of THP for the proper functioning of the MPC network, especially in the outer medulla.

The differential response of MPCs from the cortex versus medulla in both THP$^{+/+}$ and THP$^{-/-}$ to the depleting effect of clodronate is an interesting additional finding. Flow cytometry on the cortex and medulla (Supplemental Figure 10) showed small but significant differences in the phenotypic make-up of MPCs from these different renal areas, which is similar to what others have described.[59–61] Although this phenotypic difference could play a part in the resistance of the inner stripe cells to the effect of clodronate, other explanations could include the importance of the medullary milieu (as demonstrated recently by Berry *et al.*[61]), or the higher number of MPCs in the medulla, which may require a multidose regimen of clodronate.[62]

The fact that THP administration promotes the expression of MHCII on renal MPCs *in vivo* is another important finding, and is in line with *in vitro* and *ex vivo* findings by Säemann *et al.*[21] that THP causes maturation of antigen presenting cells through acquisition of MHCII. As such, THP may be a modulator of phenotypic switching toward MHCII positivity. This is supported by our observation of a concomitant decrease in MHCII^{-} renal MPCs after THP administration, which is due in part to shifting to MHCII expression. It is possible that the effect of THP on enhancing the phagocytic activity of MPCs could be related to the expression of MHCII. The fact that CD11b hi, MHCII^{-} cells were also decreased in THP$^{-/-}$ kidneys could suggest a dynamic phenotypic switching from CD11b hi MHCII^{-} to CD11b hi MHCII^{+} cells, aimed at keeping a constant pool of these MHCII^{+} cells.

The disease implications for the role of THP in regulating renal MPCs were studied in an IRI model of AKI. THP$^{-/-}$ mice have dysregulated myeloid response after IRI, with relative deficiency of MPCs and preponderance of neutrophils, even at the beginning of recovery phase (48 hours postsurgery). Data from the multiplex ELISA show a time delay in macrophage chemokine and growth factor signaling (no increase in MCSF, CCL2, or CCL4 until 48 hours post-IRI) in THP$^{-/-}$. This is in contrast to THP$^{+/+}$, where

macrophage cytokine and chemokine signaling was observed as early as 6 hours post-IRI. This could explain the disproportionate level of MPCs in $THP^{-/-}$ kidneys after AKI. Remarkably, there was a heightened level of factors involved in repair/Th2/Macrophage phenotype M2 in $THP^{+/+}$ but not $THP^{-/-}$ at 48 hours after IRI, suggesting impaired transitioning from a proinflammatory (M1) to a prohealing (M2) phenotype in $THP^{-/-}$, which was verified by flow cytometry. These findings support a previously unknown role of THP in M1/M2 phenotypic switching of macrophages. Cumulatively, these data could explain why $THP^{-/-}$ kidneys have impaired healing and persistent inflammatory response after IRI, as we reported previously.[5] In fact, MPCs are important in clearing DAMPs and neutrophils from damaged tissue.[24,28,33] Without an adequate number and activity, the MPCs are likely unable to clear DAMPs and neutrophils and, as a result, inflammation persists.[23,26,27,31] This is in agreement with earlier data from Lee *et al.*[30] showing that macrophage depletion after AKI caused persistent inflammation. In addition, an improper transition from M1 to M2 macrophage phenotype is also associated with impaired repair, which is also consistent with data by multiple other groups.[29,31,36,37] We acknowledge that this classification of macrophage phenotype is evolving, and that the M2 phenotype is now classified into additional subtypes such as 2a, 2b, and 2c. CD206 is a commonly used marker for M2 macrophages,[63,64] but future studies will be needed to determine if THP influences polarization into a specific subtype. We are also mindful that many of the cytokines/chemokines involved in phenotypic switching could be produced by epithelial cells; therefore, the effect of THP on macrophage polarization could be facilitated by an interaction with the epithelium, leading to the release of mediators favoring an M1 to M2 switch.

The physiologic relevance of THP in a repair response after AKI was further demonstrated by exogenous administration of tTHP into $THP^{-/-}$ mice. THP-treated mice 24 hours after IRI had an amelioration in the course of kidney injury, as compared with vehicle-treated mice. Administration of THP could improve kidney function in $THP^{-/-}$ by its effect on MPC number or activity. The number of $F4/80^{+}$ cells was not increased in mice treated with this single high dose of tTHP after AKI (data not shown), suggesting that the positive effect of such a one-time dose is likely due to an effect on MPC activity or phenotype switching, as we showed in Figure 11, F and G. In addition to the effect on MPCs, we cannot rule out an added protective effect of tTHP on epithelial cells, as we showed in our previous work.[5,7] Because AKI is a state of THP deficiency,[65] it is possible that administration of tTHP in $THP^{+/+}$ mice with severe AKI could also be protective, and of potential future use as a therapy to mitigate AKI. This is the subject of ongoing research in our laboratory.

In conclusion, we demonstrate a novel immunomodulatory role for THP on renal mononuclear phagocytes. Added to its positive effect on the tubular epithelium, this emergent immunomodulatory role could explain the protection conferred by THP during AKI, and could lay the foundation for modulating THP or its targets as a therapy in AKI.

Concise Methods

Mice and *In Vivo* Experiments

Animal experiments and protocols were approved by the Indianapolis Veterans Affairs Animal Care and Use Committee. Age-matched 8–12-week-old THP knockout animals (129/SvEv $THP^{-/-}$) and wild-type background strain were used as previously.[5,9,66,67] CX3CR1-EGFP (B6.129P-Cx3cr1^{tm1Litt}/J) mice were obtained from The Jackson Laboratory.

IRI using bilateral renal pedicle clamping was performed as described previously using 22-minute clamp time.[5,7] Mice were resuscitated daily with 1 cc saline to mimic clinical care. In some experiments, mice were treated with 20 μg tTHP given IP 24 hours after surgery. Sham surgery consisted of an identical procedure without application of the micro aneurysm clamps. All animals received subcutaneous analgesic

(bruprenorphine, 0.1 mg/kg) at the end of surgery and every 12 hours for 72 hours or until euthanasia. Serum creatinine was measured using capillary electrophoresis,[68] performed at the University of Texas Southwestern O'Brien Center of Excellence.

A group of $THP^{-/-}$ mice without surgery also underwent treatment with daily 10 μg injections of tTHP for 6 days before euthanasia.

In another group of mice, fluorescent beads were also injected *via* tail vein as described by Stamatiades *et al.*[50] In a pilot experiment, 20 μl of carboxylate-modified 1, 0.5, 0.2, 0.1, and 0.02 μm Fluorobeads (F8887; Invitrogen) were injected and *in vivo* phagocytosis by MPCs assessed in kidney tissue, harvested 90 minutes later (Supplemental Figure 7). We found that phagocytosis occurs for 0.2, 01, and 0.02 μm beads, but not for 0.5 and 1 μm beads, which replicates the data of Stamatiades *et al.*[50] We subsequently used 0.1 μm beads and assessed *in vivo* phagocytosis in $THP^{+/+}$ and $THP^{-/-}$. Harvested kidneys underwent immunofluorescence staining and 3D tissue cytometry as described below to quantitate bead uptake in each region of the kidney.

Other groups of $THP^{+/+}$ and $THP^{-/-}$ mice underwent injection of intravenous liposomal clodronate or empty liposomes (200 μl/animal of either Clodrosome or Encapsome suspensions by Encapsula Nano Sciences) and then underwent euthanasia 48 hours later.

Intravital imaging of the kidney was performed as described previously.[69–71] Live animal imaging was performed using an Olympus FV1000-MPE confocal/multiphoton microscope equipped with a Spectra Physics MaiTai Deep See laser and gallium arsenide detectors, with signal digitized to 12-bit resolution. The system was mounted on an Olympus Ix81 inverted microscope stand with an Olympus XLUMPLFL NA 0.95 water-immersion objective. The laser was tuned to 810-nm wavelength. Animals were placed on the stage with the exposed intact kidney placed in a coverslip-bottomed cell culture dish (HBSt-5040; Warner Instruments) bathed in isotonic saline. Two ReptiTherm pads (Zoo Med) and a heated water jacket blanket were used to maintain the temperature at 36°C. The CX3CR1-EGFP mouse was injected with Alexa568-conjugated THP intravenously (100 μg dissolved in 300 μl of 5% dextrose solution; estimated THP: Alexa dye ratio, 1:10). Hoechst 33342 (Life Technologies), dissolved in normal saline, was administered IP as a 2 mg/kg bolus 1 hour before imaging. A time-series was obtained every 9 seconds.

Another set of CX3CR1 mice were injected with Alexa 568–conjugated tTHP or vehicle and the kidneys, harvested 1 hour later, underwent flow cytometry as described below.

Cell Culture Experiments

Human Monocyte/Macrophage SC cell line (CLR-9855; ATCC) were cultured in suspension, in IMDM media supplemented with 10% FBS, 18 mM $NaHCO_3$, 0.02 mM thymidine, 0.1 mM hypoxanthine, 0.05 mM 2-mercaptoethanol, and 1× antibiotic/antimycotic solution, at 37°C in a 95% air/5% CO_2 humidified incubator and medium was replaced every 2–3 days. Cell counts and viability were done using a Countess (Life Technologies) automated system.

Tissue Sectioning, Immunofluorescence Staining, and Confocal Microscopy

Immunofluorescence staining was performed, as described previously,[7,69] on 50-μm sections of 4% paraformaldehyde–fixed kidneys from mice, and sectioned using a vibratome. The following antibodies were used for mouse tissue against the following antigens: THP (8595–0054; AbD Serotec), CD11c (sc-2867C; Santa Cruz Biotechnology, CA), MHCII (14–5321–82; eBioscience). DAPI was used for staining nuclei. Oregon Green Phalloidin (Molecular Probes, Eugene, OR) was used for staining F-actin. Confocal microscopy and image acquisition in four separate consecutive channels were performed using an Olympus Fluoview confocal microscope system (Japan).

3D Tissue Cytometry and Analysis Using Volumetric Tissue Exploration and Analysis Software

Multichannel and spectral Image acquisition was performed using a Leica SP8 confocal microscope (Germany). Volume stacks spanning the whole thickness of the tissue were taken using a 20× or a 40× objective with 0.5–1.0 μm spacing. 3D image rendering was performed using Voxx v2.09d.[72] 3D tissue cytometry was performed on image volumes using Volumetric Tissue Exploration and Analysis (VTEA), which was developed as a plugin for ImageJ/FIJI.[46,73] A prototype of VTEA can be downloaded for free with the FIJI updater (https://imagej.net/VTEA).

Immuno-Gold Electron Microscopy

Immuno-gold electron microscopy was performed as described previously[5] after staining for THP using an antibody coupled to 10 nm colloidal gold. Electron microscopy was performed using a JEOL 1200 electron microscope.

Isolation of Human Urinary THP

THP precipitation from urine of normal human donors was performed as described by Tamm and Horsfall.[74,75] Urinary THP was subsequently treated with 8 M urea for >12 hours at 4°C with tumbling. It was then concentrated on an Amicon concentrator with 10 kD MWCO (Millipore) and transferred on a Superdex 200 gel filtration column equilibrated with 30 mM phosphate buffer, pH 6.8, in 2 M urea. The column was precalibrated using specific MW markers (BioRad, CA). THP fractions were collected and the protein concentration in each fraction was determined using a spectrophotometer. Native gel electrophoresis was performed on the recovered fractions followed by denaturing and reducing SDS-PAGE. Fractions of THP isolated between 66 and 146 kD on native gel were subsequently characterized by proteomic analysis (described below), and found to be predominantly composed of a single truncated form of THP (tTHP). tTHP purified for biologic used was tested for endotoxin (Pierce LAL Chromogenic Endotoxin Quantitation Kit #88282) and underwent endotoxin removal using Pierce High Capacity Endotoxin Removal Resin (#88274). In all *in vitro* experiments, the level of endotoxin was <0.02 EU/ml. The level of endotoxin in *in vivo* dosing was <0.05 EU/dose, which conforms to the standards of preclinical pharmacology.[76]

Proteomic Characterization of tTHP

N- and C-terminal sequencing of tTHP was performed using matrix-assisted laser desorption ionization–mass spectrometry in source decay (MALDI-MS/ISD).[77] This technique does not require any special sample treatment (such as deglycosylation), and can simultaneously sequence the N and C termini for 20–50 amino acids from a small amount of protein (50–100 μg). MALDI-MS/ISD was performed through Alphalyse Inc. (Palo Alto, CA).

Immunoprecipitation of Serum THP

Normal human serum (EMD Millipore) was depleted from albumin and Igs using multiple passing on Blue Sepharose 6 (GE Healthcare) and Protein A (Pierce) resins. In some experiments, 10 ml of depleted serum underwent size exclusion chromatography on Superdex 200 resin as described above. Immunoprecipitation of THP from depleted serum or its fractions was performed in RIPA buffer using sheep anti-hTHP polyclonal antibody (R&D Systems, AF5144) at the recommended 1 μg/immunoprecipitation reaction, for >12 hours at 4°C. Binary antigen-antibody complexes were precipitated using Protein G resin (Pirece #20398), eluted with SDS-PAGE sample buffer, and subjected to electrophoresis followed by western blotting.

Western Blot

Western blot was performed as described previously.[5,65] The following primary antibodies were used: anti-THP (sc-20361; Santa Cruz Biotechnology, CA); and anti-pERK, pNFkB, and pAkt (all from Cell Signaling, MA). Secondary antibody in all instances was donkey anti–rabbit IgG-HRP (AP182P; Millipore). Blocking was performed using 5% nonfat dry milk. Blots were stripped and reprobed for actin using mouse anti-actin (cat# MAB1501; Millipore). Bands were detected by enhanced chemiluminescence (Pierce Super Signal West Pico kit, #34087) on ChemiDoc MP imaging system (BioRad, CA). Band densitometry was performed using Image J (NIH) and measurements are reported after normalization to actin.

Histochemistry and Immunohistochemical Analysis

Injury scores taking into account necrosis, dilation, and casts were performed on PAS-stained sections similar to what we described previously.[7,69] For F4/80 staining (ab2557; Abcam), 4% paraformaldehyde perfusion–fixed tissues were subsequently embedded in paraffin and processed for standard histochemistry. Negative control without primary antibody was used. Using blinded observers, cells were counted on high- (60× objective) power fields, using five fields from each kidney area per slide (two slides per kidney, and five kidneys each group). In the liposome experiments, we used the same design, but used low-power fields (20× objectives). For CD206 staining (MCA2235GA; BioRad), CD206+ cells were observed in a very patchy distribution, so the quantitation was performed on whole-kidney cross-sections (one section per kidney), imaged under a 20× objective.

Flow Cytometry on Kidneys and Livers

Flow cytometry was performed on homogenized, digested tissues as described previously.[41] In brief, kidneys or liver were homogenized and digested with collagenase, and subsequently strained using 70-μm filters. Cell counts and viability were done using a Countess automated system. A total of 5×10^6 cells from each sample were used for staining, after blocking nonspecific binding with anti-CD16/CD32 (14–0161–82; eBioscience). Flow cytometry was performed using a BD LSRII flow cytometer.

We used the following anti-mouse fluorophore-conjugated mAbs: CD45 (# 130–091–610; Miltenyi Biotech), Ly6G (# 560600; BD Bioscience), CD11b (# 48–0112–80; eBioscience), MHCII (#17–5321–82; eBioscience), F4/80 (124801–82; eBioscience), CD86 (560582; BD Pharmingen), CD206 (MCA2235F; AbD Serotec), and PI (P3566; Invitrogen) for viability.

An annexin V-FITC apoptosis kit (BMS500FI/20; eBioscience) was used to study apoptosis in SC cells. Flow Jo (version 10; tri-star) was used for flow analysis and plotting.

ELISA Assays

Multiplex cytokine/chemokine assays containing 32 prespecified analytes (Millipore # MCYTOMAG-70K-PX32) were performed on kidney lysates from $THP^{+/+}$ and $THP^{-/-}$ kidneys (n=5 per group). Values were initially reported in picograms per milligram protein/tissue after normalization to the protein concentration for each tissue. Statistical analysis is described below.

Real-Time PCR

Real-time PCR was performed as described previously[5] in Applied Biosystems ViiA7 using TaqMan Gene Expression Assays (Mm00447649_m1 for THP, Mm01324470_m1 for NGAL, all from Applied Biosystems). All expression was normalized to GADH endogenous control (4352932E for GAPDH-vic, from AB) and reported as fold-change compared with control using the Δ-Δ CT method, according to the

manufacturer's instructions.

Statistical Analyses

Unless stated otherwise, measured values of each experimental group are reported as mean±SEM. For most experiments, a *t* test was used to examine the difference in means between the experimental groups for continuous test data. A nested analysis of variance design was used for quantitation of F4/80-positive cells in immunohistochemistry. Statistical significance was determined at the 0.05 significance level. For ELISA multiplex analysis, a two-sample *t* test was used to compare the experiment test value between the two experimental groups for each of the tests. For each strain of mice, the mean difference for each test value between each time point versus sham and its 95% confidence interval were then calculated. Because each test was measured in a different metric, the test value was standardized by using the raw test value divided by its SEM. The standardized test difference and 95% confidence interval between each time point and sham for the two strains were presented in graph plots.

Disclosures

None.

Supplementary Material

Supplemental Data:

Acknowledgments

We acknowledge the assistance of the Flow Cytometry, Histopathology, and Bioplex cores at the Indiana University School of Medicine.

Veterans Affairs Merit Award, National Institutes of Health (NIH)–National Institute of Diabetes and Digestive and Kidney Diseases (NIDDK) R01DK111651, and Dialysis Clinic, Inc. research fund to T.M.E. Indiana Clinical and Translational Sciences Institute, funded in part by grant #UL1 TR001108 from the NIH, National Center for Advancing Translational Sciences, Clinical and Translational Sciences Award. NIH O'Brien Center for Advanced Renal Microscopic Analysis (NIH-NIDDK P30 DK079312) and University of Texas Southwestern George M. O'Brien Kidney Research Core Center (P30DK079328).

Footnotes

Published online ahead of print. Publication date available at www.jasn.org.

This article contains supplemental material online at http://jasn.asnjournals.org/lookup/suppl/doi:10.1681/ASN.2017040409/-/DCSupplemental.

References

1. El-Achkar TM, Wu XR.: Uromodulin in kidney injury: An instigator, bystander, or protector? Am J Kidney Dis 59: 452–461, 2012 [PMCID: PMC3288726] [PubMed: 22277744]

2. Rampoldi L, Scolari F, Amoroso A, Ghiggeri G, Devuyst O.: The rediscovery of uromodulin (Tamm-Horsfall protein): From tubulointerstitial nephropathy to chronic kidney disease. Kidney Int 80: 338–347, 2011 [PubMed: 21654721]

3. Zhu X, Cheng J, Gao J, Lepor H, Zhang ZT, Pak J, Wu XR.: Isolation of mouse THP gene promoter and demonstration of its kidney-specific activity in transgenic mice. Am J Physiol Renal Physiol 282: F608–F617, 2002 [PubMed: 11880321]

4. Bachmann S, Koeppen-Hagemann I, Kriz W.: Ultrastructural localization of Tamm-Horsfall glycoprotein (THP) in rat kidney as revealed by protein A-gold immunocytochemistry. Histochemistry 83: 531–538, 1985 [PubMed: 3910623]

5. El-Achkar TM, McCracken R, Liu Y, Heitmeier MR, Bourgeois S, Ryerse J, Wu XR.: Tamm-Horsfall protein translocates to the basolateral domain of thick ascending limbs, interstitium, and circulation during recovery from acute kidney injury. Am J Physiol Renal Physiol 304: F1066–F1075, 2013 [PMCID: PMC3625838] [PubMed: 23389456]

6. El-Achkar TM, Dagher PC.: Tubular cross talk in acute kidney injury: A story of sense and sensibility. Am J Physiol Renal Physiol 308: F1317–F1323, 2015 [PMCID: PMC4469890] [PubMed: 25877507]

7. El-Achkar TM, McCracken R, Rauchman M, Heitmeier MR, Al-Aly Z, Dagher PC, Wu XR.: Tamm-Horsfall protein-deficient thick ascending limbs promote injury to neighboring S3 segments in an MIP-2-dependent mechanism. Am J Physiol Renal Physiol 300: F999–F1007, 2011 [PMCID: PMC5504439] [PubMed: 21228114]

8. El-Achkar TM, Huang X, Plotkin Z, Sandoval RM, Rhodes GJ, Dagher PC.: Sepsis induces changes in the expression and distribution of Toll-like receptor 4 in the rat kidney. Am J Physiol Renal Physiol 290: F1034–F1043, 2006 [PubMed: 16332927]

9. El-Achkar TM, Wu XR, Rauchman M, McCracken R, Kiefer S, Dagher PC.: Tamm-Horsfall protein protects the kidney from ischemic injury by decreasing inflammation and altering TLR4 expression. Am J Physiol Renal Physiol 295: F534–F544, 2008 [PMCID: PMC5504389] [PubMed: 18495803]

10. Hato T, El-Achkar TM, Dagher PC.: Sisters in arms: Myeloid and tubular epithelial cells shape renal innate immunity. Am J Physiol Renal Physiol 304: F1243–F1251, 2013 [PMCID: PMC3651626] [PubMed: 23515715]

11. Nelson PJ, Rees AJ, Griffin MD, Hughes J, Kurts C, Duffield J.: The renal mononuclear phagocytic system. J Am Soc Nephrol 23: 194–203, 2012 [PMCID: PMC3269181] [PubMed: 22135312]

12. Kurts C, Panzer U, Anders HJ, Rees AJ.: The immune system and kidney disease: Basic concepts and clinical implications. Nat Rev Immunol 13: 738–753, 2013 [PubMed: 24037418]

13. Li L, Okusa MD.: Macrophages, dendritic cells, and kidney ischemia-reperfusion injury. Semin Nephrol 30: 268–277, 2010 [PMCID: PMC2904394] [PubMed: 20620671]

14. Muchmore AV, Decker JM.: Uromodulin: A unique 85-kilodalton immunosuppressive glycoprotein isolated from urine of pregnant women. Science 229: 479–481, 1985 [PubMed: 2409603]

15. Hession C, Decker JM, Sherblom AP, Kumar S, Yue CC, Mattaliano RJ, Tizard R, Kawashima E, Schmeissner U, Heletky S, Pingchang C, Burne CA, Shaw A, Muchmore AV, et al. .: Uromodulin (Tamm-Horsfall glycoprotein): A renal ligand for lymphokines. Science 237: 1479–1484, 1987 [PubMed: 3498215]

16. Horton JK, Davies M, Topley N, Thomas D, Williams JD.: Activation of the inflammatory response of neutrophils by Tamm-Horsfall glycoprotein. Kidney Int 37: 717–726, 1990 [PubMed: 2308259]

17. Cavallone D, Malagolini N, Serafini-Cessi F.: Binding of human neutrophils to cell-surface anchored Tamm-Horsfall glycoprotein in tubulointerstitial nephritis. Kidney Int 55: 1787–1799, 1999 [PubMed: 10231441]

18. Wimmer T, Cohen G, Saemann MD, Hörl WH.: Effects of Tamm-Horsfall protein on polymorphonuclear leukocyte function. Nephrol Dial Transplant 19: 2192–2197, 2004 [PubMed:

15266028]

19. Yu CL, Tsai CY, Lin WM, Liao TS, Chen HL, Sun KH, Chen KH.: Tamm-Horsfall urinary glycoprotein enhances monokine release and augments lymphocyte proliferation. Immunopharmacology 26: 249–258, 1993 [PubMed: 8288446]

20. Su SJ, Chang KL, Lin TM, Huang YH, Yeh TM.: Uromodulin and Tamm-Horsfall protein induce human monocytes to secrete TNF and express tissue factor. J Immunol 158: 3449–3456, 1997 [PubMed: 9120306]

21. Säemann MD, Weichhart T, Zeyda M, Staffler G, Schunn M, Stuhlmeier KM, Sobanov Y, Stulnig TM, Akira S, von Gabain A, von Ahsen U, Hörl WH, Zlabinger GJ.: Tamm-Horsfall glycoprotein links innate immune cell activation with adaptive immunity via a Toll-like receptor-4-dependent mechanism. J Clin Invest 115: 468–475, 2005 [PMCID: PMC544039] [PubMed: 15650774]

22. Borras-Cuesta F, Fedon Y, Petit-Camurdan A.: Enhancement of peptide immunogenicity by linear polymerization. Eur J Immunol 18: 199–202, 1988 [PubMed: 2450754]

23. Anders HJ, Ryu M.: Renal microenvironments and macrophage phenotypes determine progression or resolution of renal inflammation and fibrosis. Kidney Int 80: 915–925, 2011 [PubMed: 21814171]

24. Wynn TA, Chawla A, Pollard JW.: Macrophage biology in development, homeostasis and disease. Nature 496: 445–455, 2013 [PMCID: PMC3725458] [PubMed: 23619691]

25. Kolaczkowska E, Kubes P.: Neutrophil recruitment and function in health and inflammation. Nat Rev Immunol 13: 159–175, 2013 [PubMed: 23435331]

26. Thannickal VJ, Zhou Y, Gaggar A, Duncan SR.: Fibrosis: Ultimate and proximate causes. J Clin Invest 124: 4673–4677, 2014 [PMCID: PMC4347226] [PubMed: 25365073]

27. Eltzschig HK, Eckle T.: Ischemia and reperfusion--from mechanism to translation. Nat Med 17: 1391–1401, 2011 [PMCID: PMC3886192] [PubMed: 22064429]

28. Duffield JS: Macrophages in kidney repair and regeneration. J Am Soc Nephrol 22: 199–201, 2011 [PubMed: 21289208]

29. Zhang MZ, Yao B, Yang S, Jiang L, Wang S, Fan X, Yin H, Wong K, Miyazawa T, Chen J, Chang I, Singh A, Harris RC.: CSF-1 signaling mediates recovery from acute kidney injury. J Clin Invest 122: 4519–4532, 2012 [PMCID: PMC3533529] [PubMed: 23143303]

30. Lee S, Huen S, Nishio H, Nishio S, Lee HK, Choi BS, Ruhrberg C, Cantley LG.: Distinct macrophage phenotypes contribute to kidney injury and repair. J Am Soc Nephrol 22: 317–326, 2011 [PMCID: PMC3029904] [PubMed: 21289217]

31. Lech M, Gröbmayr R, Ryu M, Lorenz G, Hartter I, Mulay SR, Susanti HE, Kobayashi KS, Flavell RA, Anders HJ.: Macrophage phenotype controls long-term AKI outcomes--kidney regeneration versus atrophy. J Am Soc Nephrol 25: 292–304, 2014 [PMCID: PMC3904561] [PubMed: 24309188]

32. Stark MA, Huo Y, Burcin TL, Morris MA, Olson TS, Ley K.: Phagocytosis of apoptotic neutrophils regulates granulopoiesis via IL-23 and IL-17. Immunity 22: 285–294, 2005 [PubMed: 15780986]

33. Bratton DL, Henson PM.: Neutrophil clearance: When the party is over, clean-up begins. Trends Immunol 32: 350–357, 2011 [PMCID: PMC3151332] [PubMed: 21782511]

34. Gordy C, Pua H, Sempowski GD, He YW.: Regulation of steady-state neutrophil homeostasis by macrophages. Blood 117: 618–629, 2011 [PMCID: PMC3031484] [PubMed: 20980680]

35. Duffield JS: Macrophages and immunologic inflammation of the kidney. Semin Nephrol 30: 234–254, 2010 [PMCID: PMC2922007] [PubMed: 20620669]

36. Zhang MZ, Wang X, Wang Y, Niu A, Wang S, Zou C, Harris RC.: IL-4/IL-13-mediated polarization of renal macrophages/dendritic cells to an M2a phenotype is essential for recovery from acute kidney injury. Kidney Int 91: 375–386, 2017 [PMCID: PMC5548101] [PubMed: 27745702]

37. Griffin MD: Mononuclear phagocyte depletion strategies in models of acute kidney disease: What are they trying to tell us? Kidney Int 82: 835–837, 2012 [PubMed: 23018825]

38. George J, Lever JM, Agarwal A.: Mononuclear phagocyte subpopulations in the mouse kidney. Am J Physiol Renal Physiol 312 (4): F640–F646, 2017 [PMCID: PMC5504394] [PubMed: 28100500]

39. Heng TS, Painter MW; Immunological Genome Project Consortium .: The Immunological Genome Project: Networks of gene expression in immune cells. Nat Immunol 9: 1091–1094, 2008 [PubMed: 18800157]

40. Kawakami T, Lichtnekert J, Thompson LJ, Karna P, Bouabe H, Hohl TM, Heinecke JW, Ziegler SF, Nelson PJ, Duffield JS.: Resident renal mononuclear phagocytes comprise five discrete populations with distinct phenotypes and functions. J Immunol 191: 3358–3372, 2013 [PMCID: PMC3808972] [PubMed: 23956422]

41. Micanovic R, Chitteti BR, Dagher PC, Srour EF, Khan S, Hato T, Lyle A, Tong Y, Wu XR, El-Achkar TM.: Tamm-Horsfall protein regulates granulopoiesis and systemic neutrophil homeostasis. J Am Soc Nephrol 26: 2172–2182, 2015 [PMCID: PMC4552115] [PubMed: 25556169]

42. Serafini-Cessi F, Malagolini N, Cavallone D.: Tamm-Horsfall glycoprotein: Biology and clinical relevance. Am J Kidney Dis 42: 658–676, 2003 [PubMed: 14520616]

43. Schaeffer C, Santambrogio S, Perucca S, Casari G, Rampoldi L.: Analysis of uromodulin polymerization provides new insights into the mechanisms regulating ZP domain-mediated protein assembly. Mol Biol Cell 20: 589–599, 2009 [PMCID: PMC2626557] [PubMed: 19005207]

44. Santambrogio S, Cattaneo A, Bernascone I, Schwend T, Jovine L, Bachi A, Rampoldi L.: Urinary uromodulin carries an intact ZP domain generated by a conserved C-terminal proteolytic cleavage. Biochem Biophys Res Commun 370: 410–413, 2008 [PubMed: 18375198]

45. Bokhove M, Nishimura K, Brunati M, Han L, de Sanctis D, Rampoldi L, Jovine L.: A structured interdomain linker directs self-polymerization of human uromodulin. Proc Natl Acad Sci U S A 113: 1552–1557, 2016 [PMCID: PMC4760807] [PubMed: 26811476]

46. Winfree S, Khan S, Micanovic R, Eadon MT, Kelly KJ, Sutton TA, Phillips CL, Dunn KW, El-Achkar TM.: Quantitative three-dimensional tissue cytometry to study kidney tissue and resident immune cells. J Am Soc Nephrol 28: 2108–2118, 2017 [PMCID: PMC5491289] [PubMed: 28154201]

47. Li L, Huang L, Sung SS, Vergis AL, Rosin DL, Rose CE Jr, Lobo PI, Okusa MD.: The chemokine receptors CCR2 and CX3CR1 mediate monocyte/macrophage trafficking in kidney ischemia-reperfusion injury. Kidney Int 74: 1526–1537, 2008 [PMCID: PMC2652647] [PubMed: 18843253]

48. Soos TJ, Sims TN, Barisoni L, Lin K, Littman DR, Dustin ML, Nelson PJ.: CX3CR1+ interstitial dendritic cells form a contiguous network throughout the entire kidney. Kidney Int 70: 591–596, 2006 [PubMed: 16760907]

49. Danenberg HD, Fishbein I, Gao J, Mönkkönen J, Reich R, Gati I, Moerman E, Golomb G.: Macrophage depletion by clodronate-containing liposomes reduces neointimal formation after balloon

injury in rats and rabbits. Circulation 106: 599–605, 2002 [PubMed: 12147543]

50. Stamatiades EG, Tremblay ME, Bohm M, Crozet L, Bisht K, Kao D, Coelho C, Fan X, Yewdell WT, Davidson A, Heeger PS, Diebold S, Nimmerjahn F, Geissmann F.: Immune monitoring of trans-endothelial transport by kidney-resident macrophages. Cell 166: 991–1003, 2016 [PMCID: PMC4983224] [PubMed: 27477514]

51. Paragas N, Qiu A, Zhang Q, Samstein B, Deng SX, Schmidt-Ott KM, Viltard M, Yu W, Forster CS, Gong G, Liu Y, Kulkarni R, Mori K, Kalandadze A, Ratner AJ, Devarajan P, Landry DW, D'Agati V, Lin CS, Barasch J.: The Ngal reporter mouse detects the response of the kidney to injury in real time. Nat Med 17: 216–222, 2011 [PMCID: PMC3059503] [PubMed: 21240264]

52. Risch L, Lhotta K, Meier D, Medina-Escobar P, Nydegger UE, Risch M.: The serum uromodulin level is associated with kidney function. Clin Chem Lab Med 52: 1755–1761, 2014 [PubMed: 24933630]

53. Delgado GE, Kleber ME, Scharnagl H, Krämer BK, März W, Scherberich JE.: Serum uromodulin and mortality risk in patients undergoing coronary angiography. J Am Soc Nephrol 28: 2201–2210, 2017 [PMCID: PMC5491294] [PubMed: 28242751]

54. Leiherer A, Muendlein A, Saely CH, Kinz E, Brandtner EM, Fraunberger P, Drexel H.: Serum uromodulin is associated with impaired glucose metabolism. Medicine (Baltimore) 96: e5798, 2017 [PMCID: PMC5293418] [PubMed: 28151855]

55. Feinberg H, Uitdehaag JC, Davies JM, Wallis R, Drickamer K, Weis WI.: Crystal structure of the CUB1-EGF-CUB2 region of mannose-binding protein associated serine protease-2. EMBO J 22: 2348–2359, 2003 [PMCID: PMC155994] [PubMed: 12743029]

56. Jovine L, Janssen WG, Litscher ES, Wassarman PM.: The PLAC1-homology region of the ZP domain is sufficient for protein polymerisation. BMC Biochem 7: 11, 2006 [PMCID: PMC1479692] [PubMed: 16600035]

57. Wilburn DB, Swanson WJ.: The "ZP domain" is not one, but likely two independent domains. Mol Reprod Dev 84: 284–285, 2017 [PMCID: PMC5395334] [PubMed: 28176401]

58. Cavallone D, Malagolini N, Monti A, Wu XR, Serafini-Cessi F.: Variation of high mannose chains of Tamm-Horsfall glycoprotein confers differential binding to type 1-fimbriated Escherichia coli. J Biol Chem 279: 216–222, 2004 [PubMed: 14570881]

59. Chessa F, Mathow D, Wang S, Hielscher T, Atzberger A, Porubsky S, Gretz N, Burgdorf S, Gröne HJ, Popovic ZV.: The renal microenvironment modifies dendritic cell phenotype. Kidney Int 89: 82–94, 2016 [PubMed: 26466317]

60. Hochheiser K, Heuser C, Krause TA, Teteris S, Ilias A, Weisheit C, Hoss F, Tittel AP, Knolle PA, Panzer U, Engel DR, Tharaux PL, Kurts C.: Exclusive CX3CR1 dependence of kidney DCs impacts glomerulonephritis progression. J Clin Invest 123: 4242–4254, 2013 [PMCID: PMC3784547] [PubMed: 23999431]

61. Berry MR, Mathews RJ, Ferdinand JR, Jing C, Loudon KW, Wlodek E, Dennison TW, Kuper C, Neuhofer W, Clatworthy MR.: Renal sodium gradient orchestrates a dynamic antibacterial defense zone. Cell 170: 860– 874 e819, 2017 [PubMed: 28803730]

62. Kitamoto K, Machida Y, Uchida J, Izumi Y, Shiota M, Nakao T, Iwao H, Yukimura T, Nakatani T, Miura K.: Effects of liposome clodronate on renal leukocyte populations and renal fibrosis in murine obstructive nephropathy. J Pharmacol Sci 111: 285–292, 2009 [PubMed: 19893275]

63. Biswas SK, Mantovani A.: Macrophage plasticity and interaction with lymphocyte subsets: Cancer as a paradigm. Nat Immunol 11: 889–896, 2010 [PubMed: 20856220]

64. Olsson A, Nakhlé J, Sundstedt A, Plas P, Bauchet AL, Pierron V, Bruetschy L, Deronic A, Törngren M, Liberg D, Schmidlin F, Leanderson T.: Tasquinimod triggers an early change in the polarization of tumor associated macrophages in the tumor microenvironment. J Immunother Cancer 3: 53, 2015 [PMCID: PMC4678646] [PubMed: 26673090]

65. Heitmeier M, McCracken R, Micanovic R, Khan S, El-Achkar TM.: The role of tumor necrosis factor alpha in regulating the expression of Tamm-Horsfall Protein (uromodulin) in thick ascending limbs during kidney injury. Am J Nephrol 40: 458–467, 2014 [PMCID: PMC5844861] [PubMed: 25503683]

66. Mo L, Huang HY, Zhu XH, Shapiro E, Hasty DL, Wu XR.: Tamm-Horsfall protein is a critical renal defense factor protecting against calcium oxalate crystal formation. Kidney Int 66: 1159–1166, 2004 [PubMed: 15327412]

67. Mo L, Zhu XH, Huang HY, Shapiro E, Hasty DL, Wu XR.: Ablation of the Tamm-Horsfall protein gene increases susceptibility of mice to bladder colonization by type 1-fimbriated Escherichia coli. Am J Physiol Renal Physiol 286: F795–F802, 2004 [PubMed: 14665435]

68. Paroni R, Fermo I, Cighetti G, Ferrero CA, Carobene A, Ceriotti F.: Creatinine determination in serum by capillary electrophoresis. Electrophoresis 25: 463–468, 2004 [PubMed: 14760638]

69. El-Achkar TM, Plotkin Z, Marcic B, Dagher PC.: Sepsis induces an increase in thick ascending limb Cox-2 that is TLR4 dependent. Am J Physiol Renal Physiol 293: F1187–F1196, 2007 [PubMed: 17634395]

70. Hato T, Winfree S, Kalakeche R, Dube S, Kumar R, Yoshimoto M, Plotkin Z, Dagher PC.: The macrophage mediates the renoprotective effects of endotoxin preconditioning. J Am Soc Nephrol 26 (6): 1347–1362, 2015 [PMCID: PMC4446880] [PubMed: 25398784]

71. Kalakeche R, Hato T, Rhodes G, Dunn KW, El-Achkar TM, Plotkin Z, Sandoval RM, Dagher PC.: Endotoxin uptake by S1 proximal tubular segment causes oxidative stress in the downstream S2 segment. J Am Soc Nephrol 22: 1505–1516, 2011 [PMCID: PMC3148705] [PubMed: 21784899]

72. Clendenon JL, Phillips CL, Sandoval RM, Fang S, Dunn KW.: Voxx: A PC-based, near real-time volume rendering system for biological microscopy. Am J Physiol Cell Physiol 282: C213–C218, 2002 [PubMed: 11742814]

73. Winfree S, Ferkowicz MJ, Dagher PC, Kelly KJ, Eadon MT, Sutton TA, Markel TA, Yoder MC, Dunn KW, El-Achkar TM.: Large-scale 3-dimensional quantitative imaging of tissues: State-of-the-art and translational implications. Transl Res 189: 1–12, 2017 [PMCID: PMC5659947] [PubMed: 28784428]

74. Tamm I, Horsfall FL Jr.: Characterization and separation of an inhibitor of viral hemagglutination present in urine. Proc Soc Exp Biol Med 74: 106–108, 1950 [PubMed: 15430405]

75. Tamm I, Horsfall FL Jr.: A mucoprotein derived from human urine which reacts with influenza, mumps, and Newcastle disease viruses. J Exp Med 95: 71–97, 1952 [PMCID: PMC2212053] [PubMed: 14907962]

76. Malyala P, Singh M.: Endotoxin limits in formulations for preclinical research. J Pharm Sci 97: 2041–2044, 2008 [PubMed: 17847072]

77. Debois D, Bertrand V, Quinton L, De Pauw-Gillet MC, De Pauw E.: MALDI-in source decay applied to mass spectrometry imaging: A new tool for protein identification. Anal Chem 82: 4036–4045, 2010 [PubMed: 20397712]

Figures and Tables

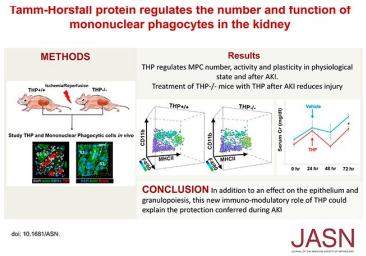
Tamm-Horsfall protein regulates the number and function of mononuclear phagocytes in the kidney
METHODS
Ischemia/Reperfusion
THP+/+
THP-/-
Study THP and Mononuclear Phagocytic cells in vivo
Results
THP regulates MPC number, activity and plasticity in physiological state and after AKI.
Treatment of THP-/- mice with THP after AKI reduces injury
THP+/+
THP-/-
CD11b
MHCII
Vehicle
THP
Serum Cr (mg/dl)
0 hr
24 hr
48 hr
72 hr
CONCLUSION In addition to an effect on the epithelium and granulopoiesis, this new immuno-modulatory role of THP could explain the protection conferred during AKI
doi: 10.1681/ASN.
JASN

Figure 1.

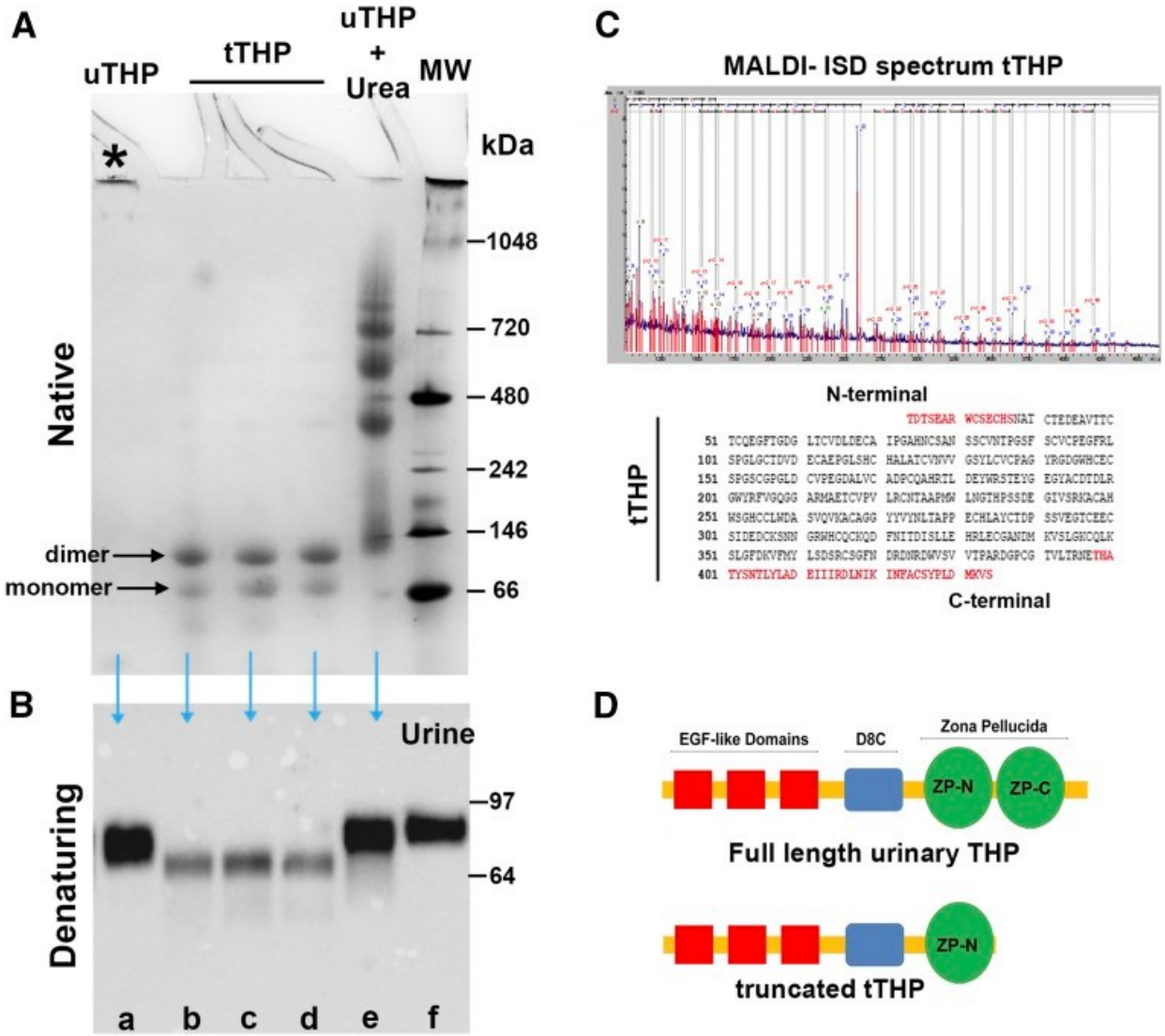

Characterization of urinary THP. (A) Electrophoresis under native conditions of various forms of THP: urinary THP purified by the method of Tamm and Horsfall (uTHP, lane a), truncated THP isolated by size exclusion chromatography (tTHP, lanes b–d), and urinary THP treated with 8 M urea (lane e). Molecular mass markers are shown in lane f. Aggregated uTHP does not undergo electrophoresis under native conditions (asterisk). Two bands of tTHP corresponding to a monomer and a dimer are observed. Multiple high–molecular mass aggregates are observed in lane e, reflecting the chaotropic effect of urea on THP multimers. (B) Western blotting of SDS-PAGE applied on to the same forms of THP is seen, with the addition of a urine sample in lane f. tTHP is now reduced to a single band, which is in the range of 64–68 kD. (C) Proteomic characterization of tTHP using MALDI-ISD maps the C-terminal sequence of tTHP to a region ending in amino acid 434, which is in the region within the two subdomains (ZP-N and ZP-C) of the ZP, with an estimated molecular mass around 65 kD. (D) Schematic representation of full-length THP and tTHP, underscoring the site of truncation at the ZP domain. MALDI-ISD, matrix-assisted laser desorption ionization-in source decay.

Figure 2.

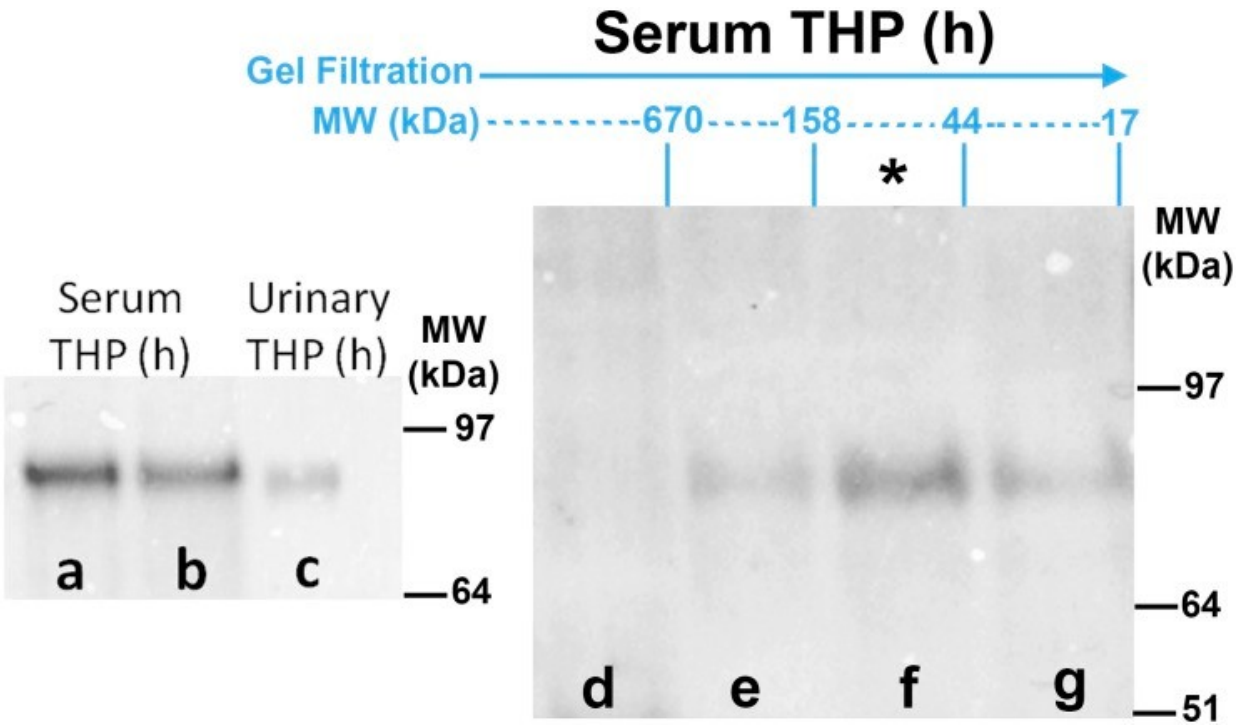

Characterization of THP in the circulation. Western blots for THP after immuno-precipitation are shown in all lanes except lane c. Lanes a and b demonstrate that THP in the human (h) serum has a comparable molecular mass (approximately 85–90 kD) to full-length human urinary THP (lane c). Lanes d–g show immuno-blotting for THP on different fractions of serum, separated according to molecular mass by size exclusion chromatography. THP is predominantly present in the fractions between 44 and 158 kD (lane f, asterisk), proving that THP in the circulation is mostly in the monomeric form.

Figure 3.

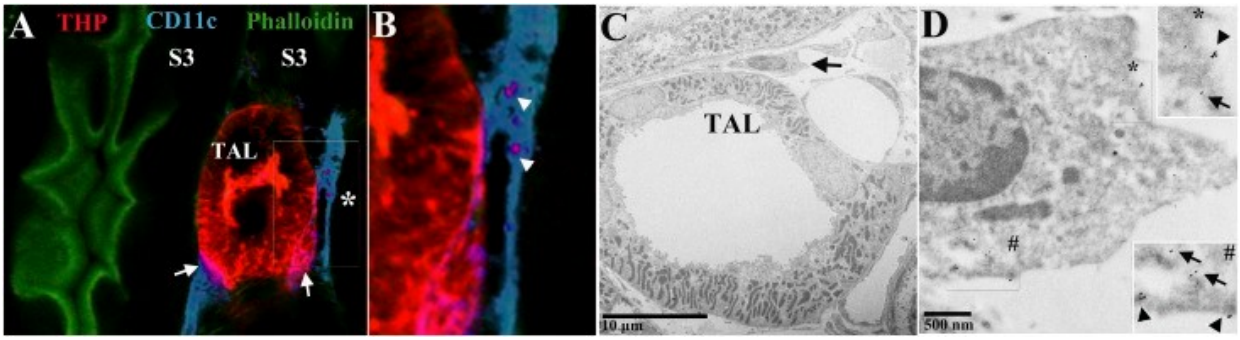

THP in the kidney interstitium colocalizes with MPCs. (A) Confocal microscopy image of a kidney field in the outer medulla viewed under a 40× objective, showing a TAL intricately associated with resident mononuclear phagocytic $CD11c^{+}$ cell (blue). Arrows show areas of colocalization at the basolateral domain of TAL. (B) The area marked by the asterisk is enlarged, where two distinct areas within a $CD11C^{+}$ cell also show THP staining, suggesting THP uptake by these cells. (C) Electron micrograph of a TAL and a mononuclear cell in the outer medulla, whereby THP is labeled with gold particles. (D) The area marked by the arrow in (C) is enlarged, where gold-labeled THP is observed at the plasma membrane (arrowheads) and within the cytoplasm (arrows). The insets are enlarged areas marked by the asterisk and the pound sign.

Figure 4.

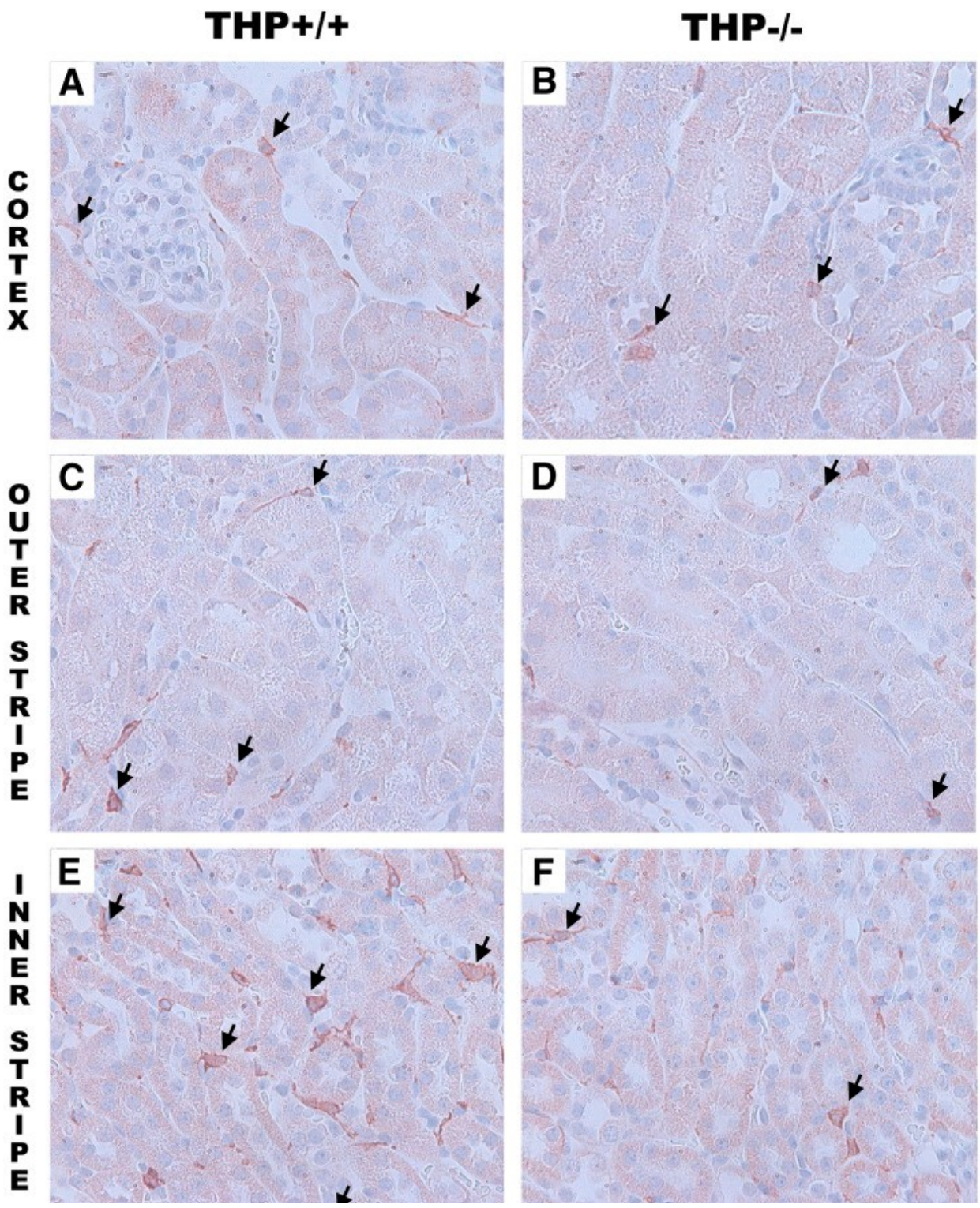

Open in a separate window

Immunohistochemistry for F4/80 in $THP^{+/+}$ and $THP^{-/-}$ kidneys. (A–H) Panels are representative images (40× objective) of sections (two sections/kidney, five kidneys per group) encompassing all areas within the kidney from $THP^{+/+}$ and $THP^{-/-}$ mice. Arrows show F4/80-stained cells in various areas within the kidney. $THP^{-/-}$ kidneys have significant depletion of $F4/80^{+}$ cells in the outer medulla. (I) Quantitation of $F4/80^{+}$ cells in each renal zone (five fields for each renal zone/section). Bar graphs are mean±SEM. Asterisk represents statistical significance between the two strains ($P<0.05$).

Figure 5.

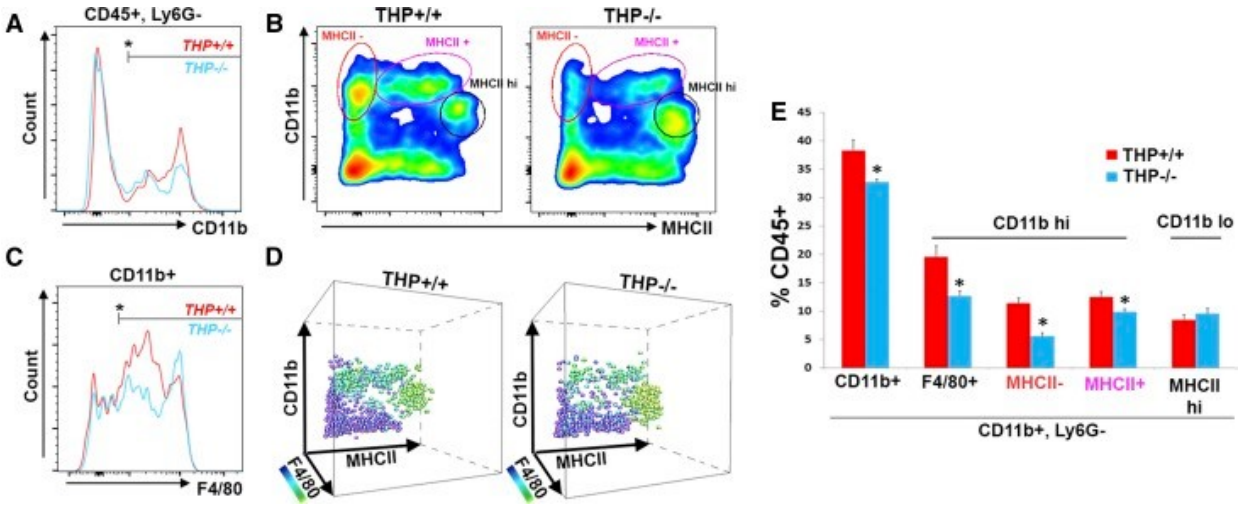

Flow cytometry detects depletion of specific MPC population in $THP^{-/-}$ compared with $THP^{+/+}$ kidneys. (A) Representative flow cytometry normalized cell count histograms showing the distribution of CD11b within $CD45^{+}Ly6G^{-}$ gated cells, in $THP^{+/+}$ versus $THP^{-/-}$ kidneys. Bar mark denotes the positive range in the histogram. (B) Scatter plots of these cells gated for according to CD11b and MHCII intensity. (C) Distribution of F4/80 among $CD11b^{+}$ cells. (D) 3D visualization of the plots from (B), with the added dimension of F4/80. The colorization corresponds to F4/80 positivity as shown in the scale bar. (E) The corresponding quantitation of the gated cells as percentage of $CD45^{+}$ cells. The MPC cell population that is reduced in number in $THP^{-/-}$ is CD11b hi and $F4/80^{+}$. Asterisk represents a statistically significant difference between $THP^{+/+}$ and $THP^{-/-}$ (n=5 per group, P<0.05). hi, high; lo, low.

Figure 6.

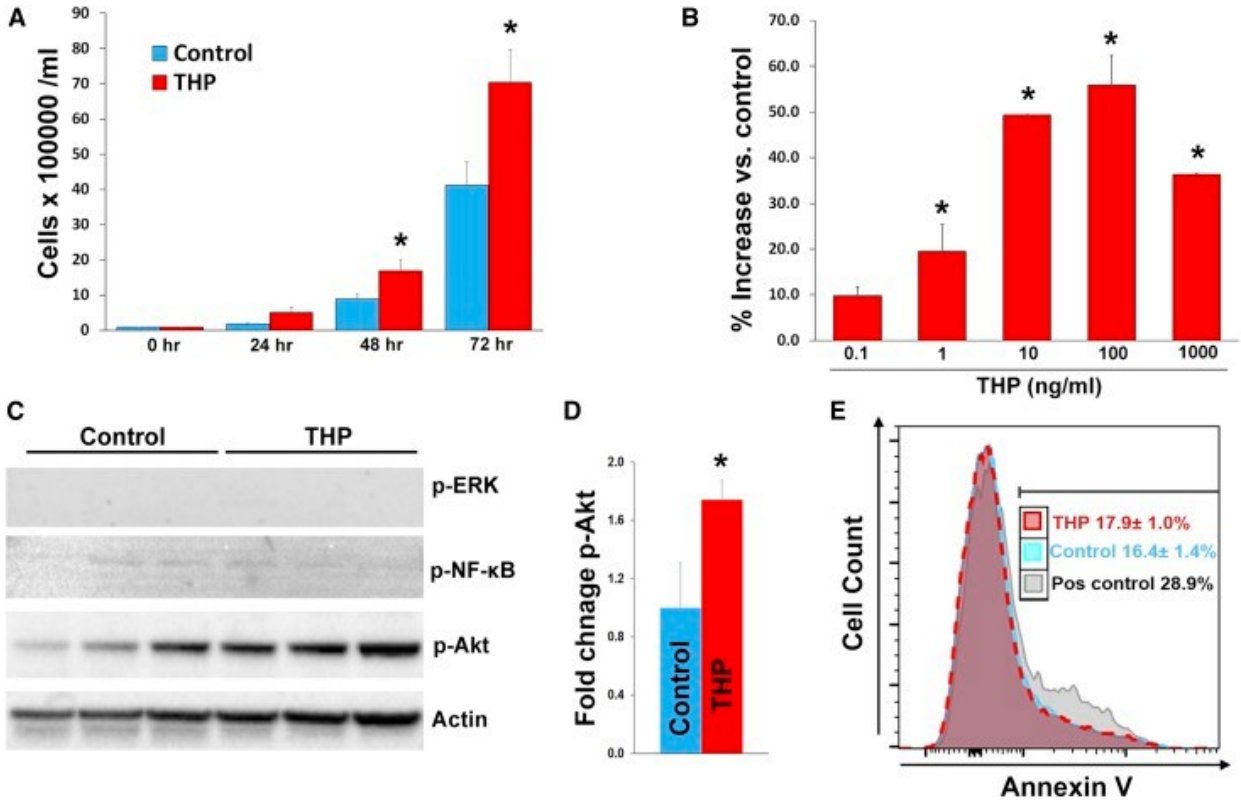

THP causes proliferation of SC macrophage cells and activation of Akt. Bar graphs are mean±SEM. Graph (A) shows the effect of tTHP (1 μg/ml) on the proliferation of SC cells using an automated viability assay (six replicates per group). There was significant difference of tTHP-treated versus vehicle starting 48 hours after treatment. In (B), we measured the effect of different concentrations of tTHP on cell proliferation at 48 hours. We observed a dose-dependent increase in cell number compared with control-treated cells. We then probed for the activation of ERK, NF-κB, and Akt using western blot for the phosphorylated active forms. Only Akt showed significant activation with THP treatment, which (D) was confirmed by band densitometry. (E) Flow cytometry–based PI/annexin V apoptosis assay on SC cells treated with tTHP or control. A positive control using LPS treatment of SC cells is also shown. There was no change in the rate of apoptosis (PI^-, annexin V^+) between tTHP- and vehicle-treated SC cells. *denotes statistical significance between control and THP treatment $P<0.05$. Pos, positive; vs., versus.

Figure 7.

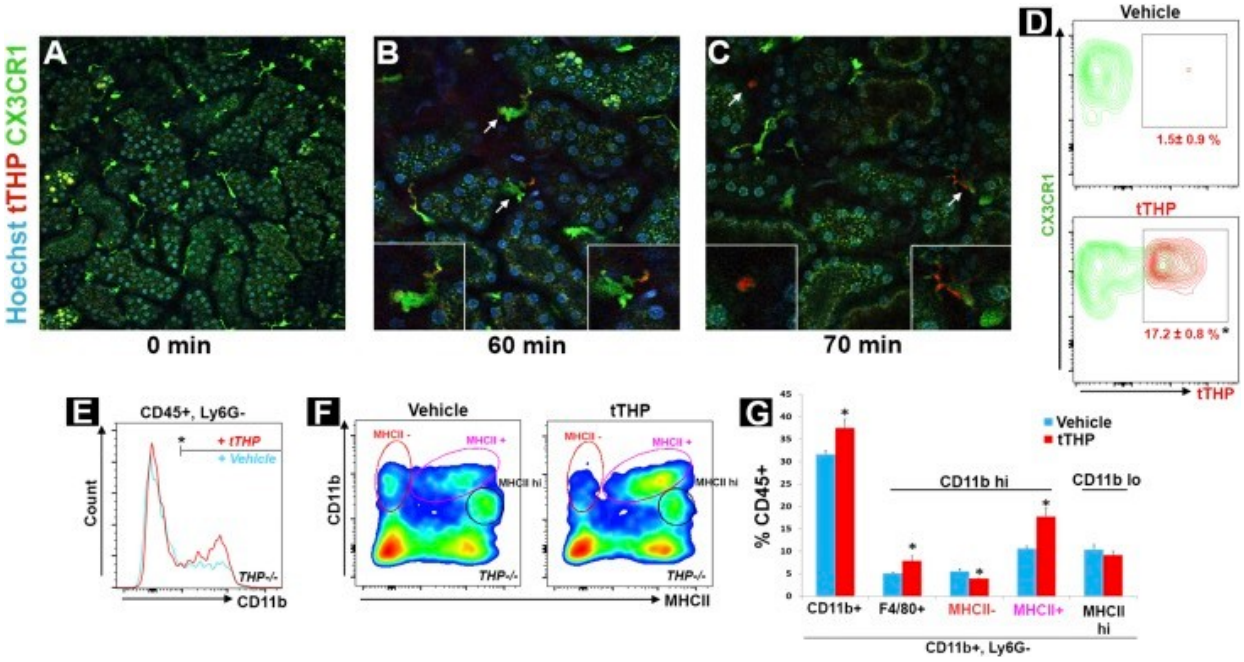

Treatment with exogenous tTHP increases the number of mononuclear phagocytes. (A–C) show intravital imaging of the kidney cortex in CX3CR1-GFP^{+} mice, showing resident dendritic and macrophage cells labeled in green, (A) before (20× objective) and (B and C) after (60× objective) injection of tTHP labeled with Alexa 568 in red. THP was observed in the peritubular circulation and interstitium as early as 30 minutes postinjection (data not shown), and is taken up by dendritic cells and macrophages starting at 60 minutes. Insets show enlargement of the cells indicated by the arrows. Macrophages have a characteristic shape (left inset in C) and a high degree of mobility (see Supplemental Video). (D) Representative flow cytometry contour plot showing the distribution of tTHP uptake in CX3CR-GFP^{+} cells 1 hour after injection compared with vehicle (n=4 per group). The mean±SEM are shown for each group, and the asterisk denotes statistical significance between the groups, P<0.05. (E) Representative histogram showing the distribution of CD11b within CD45^{+}Ly6G^{-} gated cells, in kidneys from THP$^{-/-}$ treated with THP or vehicle as described in the Concise Methods. (F) Scatter plots of these cells gated for according to CD11b and MHCII intensity, and (G) the corresponding quantitation of the gated cells as percentage of CD45+ cells. Asterisks represent a statistically significant difference between groups (n=5 per group, P<0.05). hi, high; lo, low.

Figure 8.

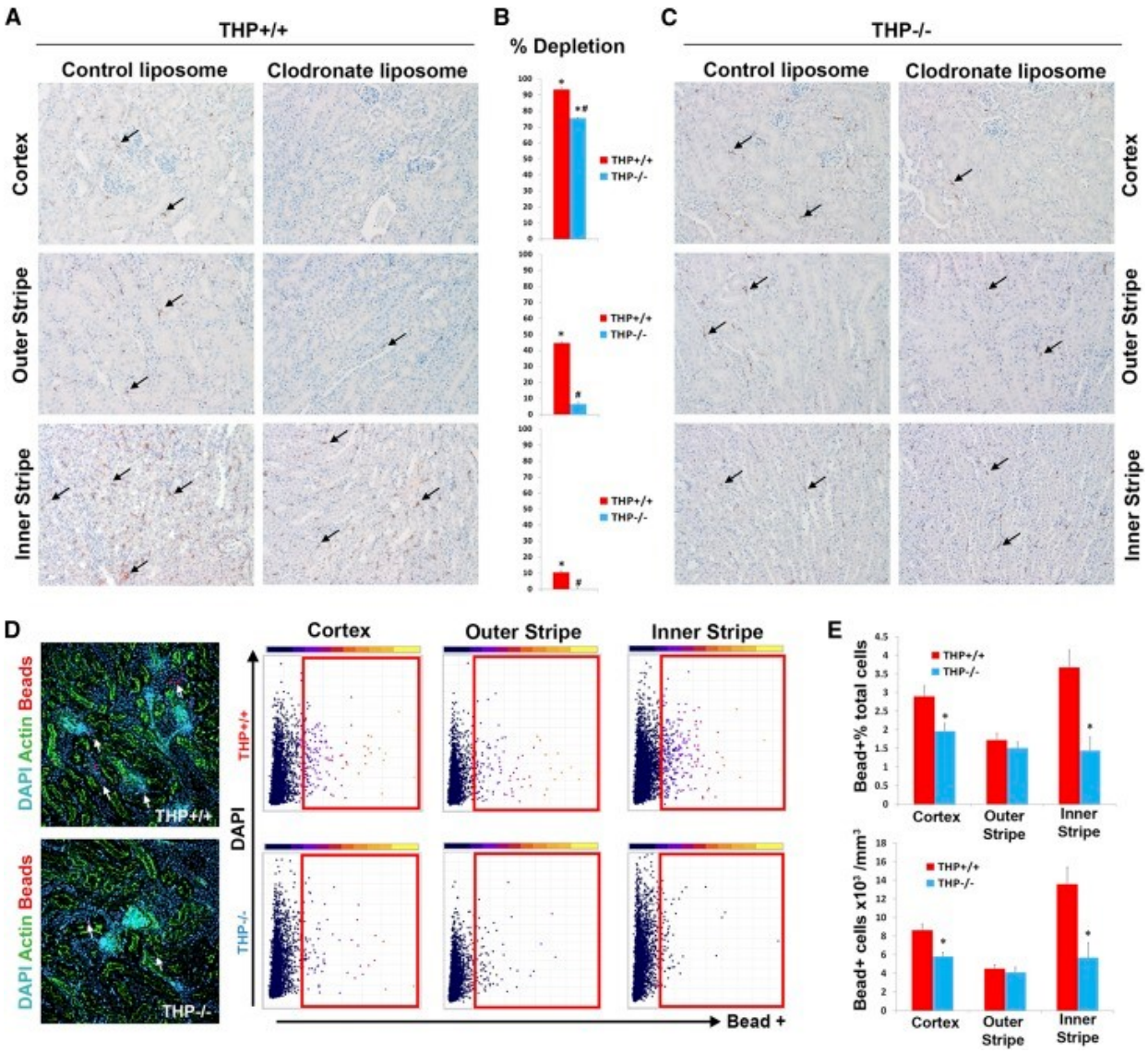

Impaired phagocytic activity of renal MPCs *in vivo* with THP deficiency. (A and C) F4/80 immunohistochemistry (arrows pointing to F4/80^{+} cells) of representative kidney sections from THP$^{+/+}$ or THP$^{-/-}$ mice (n=5 per group/treatment) treated with empty liposomes or with clodronate liposomes, respectively. (B) Bar graphs showing the percentage of F4/80 macrophage depletion with clodronate versus empty liposome of each mouse genotype in different areas of the kidney. *Statistical significance for clodronate versus control liposome; # denotes significance between THP$^{+/+}$ and THP$^{-/-}$ (P<0.05). (D) (left) Representative z projections of image stacks spanning 50 μm, imaged with spectral confocal microscopy (20× objective), from kidney sections of THP$^{+/+}$ and THP$^{-/-}$ mice, 90 minutes after intravenous injections of fluorescent beads. 3D tissue cytometry scatter plots are shown from each area of the kidney, with gates indicating bead+ cells. (E) Quantitation of bead+ cell abundance and density. Asterisk denotes statistical significance between the two groups (n=5 per group).

Figure 9.

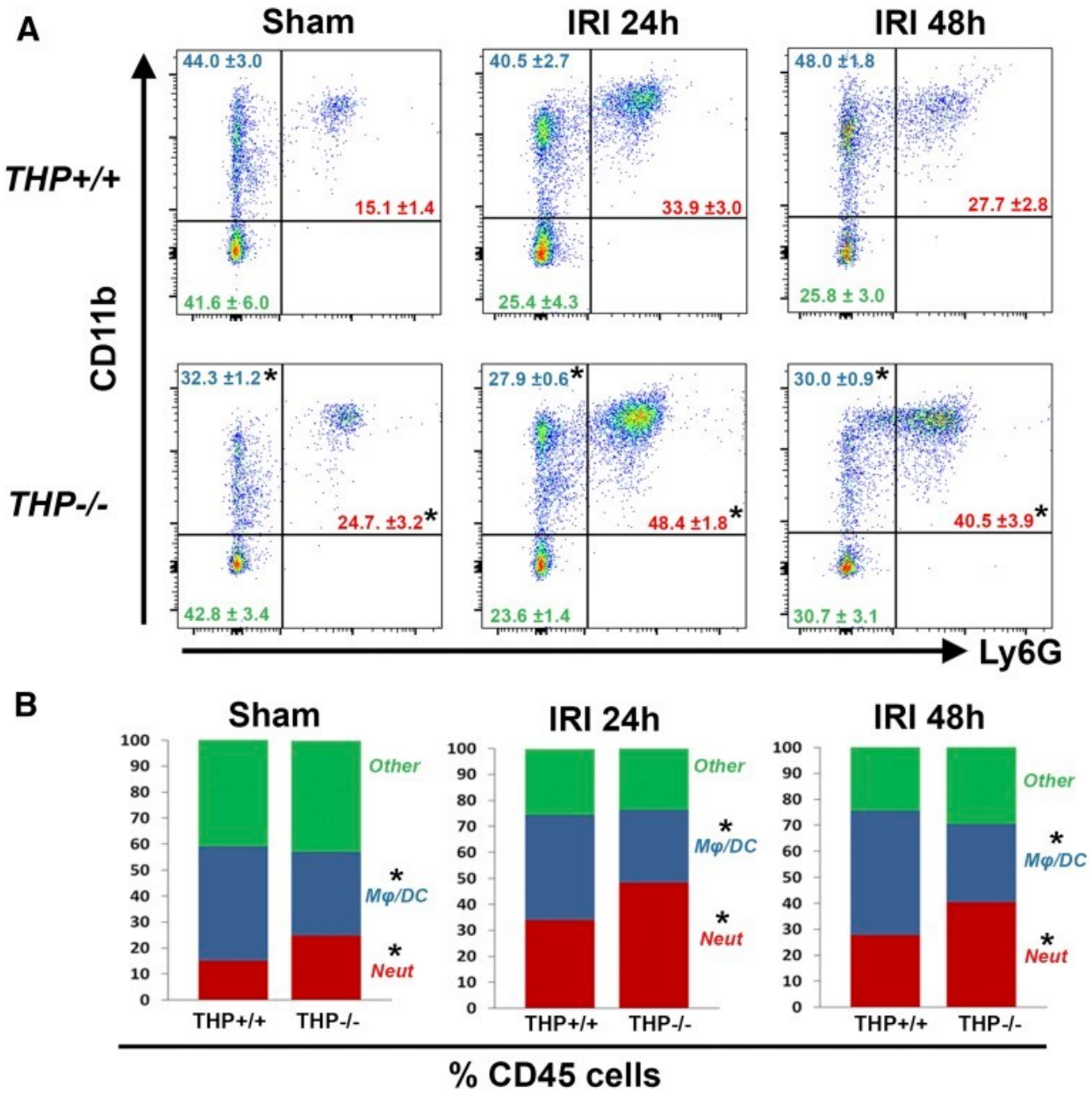

Open in a separate window

Flow cytometry for myeloid cells in $THP^{+/+}$ and $THP^{-/-}$ kidneys during AKI. (A) The fluorescence distribution of CD11b and Ly6G in $CD45^{+}$ gated cells. Neutrophils were defined as $CD45^{+}$ $CD11b^{+}$ $Ly6G^{+}$, whereas macrophages/dendritic cells Mφ/DC were defined as $CD45^{+}$ $CD11b^{+}$ $Ly6G^{-}$. The distribution of cells as a percentage of $CD45^{+}$ cells is shown in each quadrant, and (B) displayed using stacked bar graphs. Asterisk denotes statistical significance between $THP^{+/+}$ and $THP^{-/-}$ ($P<0.05$, $n=5$/group per time point). Neut, neutrophils.

Figure 10.

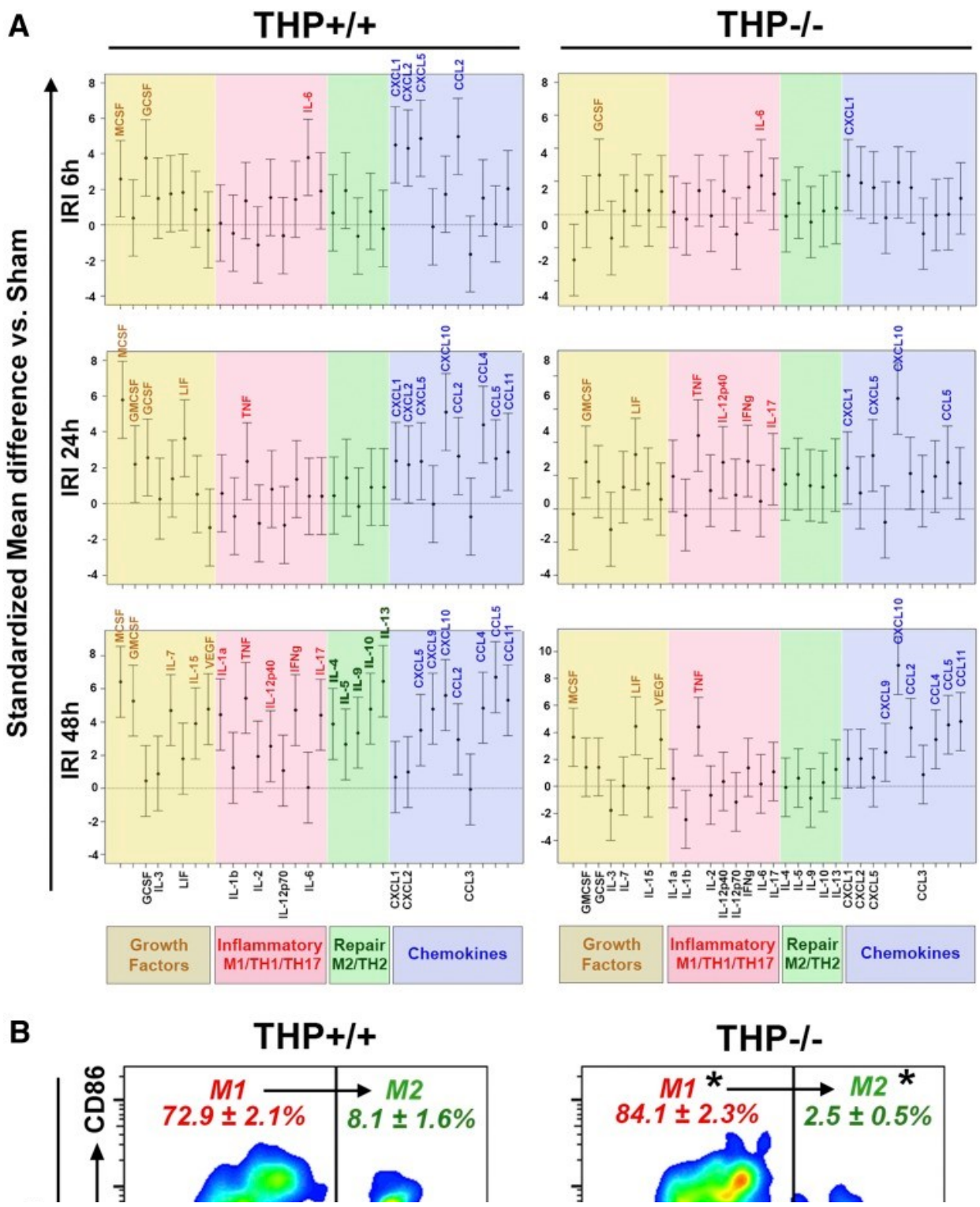

Open in a separate window

Impaired M1 to M2 macrophage phenotype switching in THP$^{-/-}$ mice during AKI. (A) Cytokine/chemokine multiplex ELISA array was performed on kidneys from THP$^{-/-}$ and THP$^{+/+}$ at various time points after IRI surgery and compared with sham for each strain (n=5 per group at each timepoint). Graphs in (A) show standardized mean differences for each analyte compared with sham for each strain. Analytes are grouped on the basis of their biologic function. Statistical significance between IRI and sham for each timepoint is present when the name of the corresponding analyte is displayed on top of the confidence interval bracket. (B) Flow cytometry for M1 and M2 markers (CD86 and CD206, respectively),

performed on kidney homogenates from $THP^{+/+}$ and $THP^{-/-}$ mice, 48 hours after IRI and gated on macrophages ($CD45^{+}$, $Ly6G^{-}$, $F4/80^{+}$). Percentages of macrophages for each subgated population (mean±SEM; n=5/group) are displayed in the corresponding quadrants. Asterisk (*) denotes statistical significance between $THP^{+/+}$ and $THP^{-/-}$ (P<0.05). vs., versus.

Figure 11.

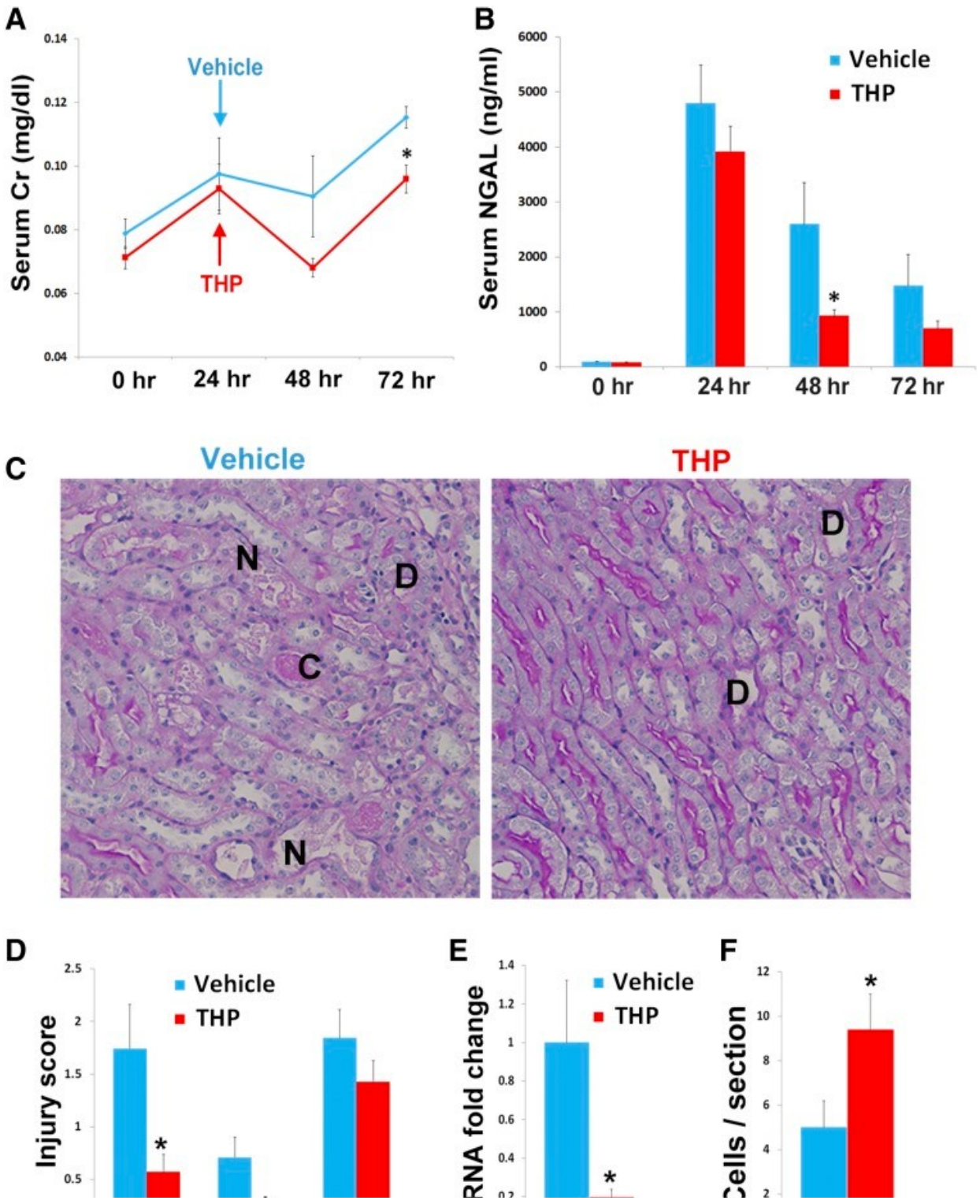

Open in a separate window

Administration of tTHP after IRI ameliorates injury: THP$^{-/-}$ mice were treated 24 hours after IRI with THP or vehicle. (A) Serum Cr and (B) NGAL were measured at baseline and after injury. THP-treated mice had a reduction in subsequent injury compared with vehicle. (C and D) Histologic assessment at 72 hours also shows improvement of injury (assessed by necrosis [N], casts [C], and dilation [D]). (E) This was quantitated using an injury scoring system. (D) NGAL mRNA after THP- or vehicle-treated mice. (F) Quantitative analysis of CD206^{+} cells (mean±SEM per kidney cross-section), and (G) representative images of CD206 immunohistochemitry. The insets are enlarged views of the areas marked within the

boxes. Asterisk denotes statistical significance ($P<0.05$) between the two groups. $n=7–8$ per group. Serum Cr, creatinine.

Articles from Journal of the American Society of Nephrology : JASN are provided here courtesy of **American Society of Nephrology**